

A conceptual and numerical model of fluid flow and heat transport in the Topusko hydrothermal system

Mirja Pavić¹, Marco Pola¹, Bojan Matoš^{2,*}, Katarina Mišić², Ivan Kosović¹, Ivica Pavičić² and Staša Borović¹

¹ Croatian Geological Survey, Sachsova 2, 10000 Zagreb, Croatia

² University of Zagreb, Faculty of Mining, Geology and Petroleum Engineering, Pierottijeva ulica 6, 10000 Zagreb, Croatia;
(*corresponding author: bojan.matos@rgn.unizg.hr)

doi: 10.4154/gc.2024.14



Article history:

Manuscript received: May 16, 2024

Revised manuscript accepted: June 11, 2024

Available online: August 28, 2024

Abstract

A comprehensive understanding of hydrothermal systems is often obtained through the integration of conceptual and numerical modelling. This integrated approach provides a structured framework for the reconstruction and quantification of fluid dynamics in the reservoir, thereby facilitating informed decision-making for sustainable utilisation and environmental protection of the hydrothermal system. In this study, an updated conceptual model of the Topusko hydrothermal system (THS), central Croatia, is proposed based on structural, geochemical, and hydrogeological analyses. The stratigraphic sequence and the structural framework of the THS were defined based on geological maps and field investigations. As depicted by hydrochemical and isotope analyses, the thermal waters in the Topusko system (temperatures < 65 °C) are of meteoric origin and circulate in a carbonate aquifer. The THS receives diffuse recharge approximately 13 km S of Topusko, where Triassic carbonates crop out. Gravity-driven regional groundwater circulation is favoured by regional thrusts that tectonically uplifted Palaeozoic rocks of low permeability. These structures confine the fluid flow in the permeable, fractured and karstified Triassic carbonates, favouring the northward circulation of the water. A regional anticline lifts the aquifer closer to the surface in Topusko. Open fractures in the anticline hinge zone increase the fracturing and permeability field of the aquifer, promoting the rapid upwelling of thermal water resulting in the Topusko thermal springs. Numerical simulations of fluid flow and heat transport corroborate the proposed conceptual model. In particular, a thermal anomaly was modelled in the Topusko subsurface with temperature values of 31.3 °C and 59.5 °C at the surface and at the base of the thermal aquifer, respectively, approaching the field observations. These findings show that the circulation of Topusko thermal water is influenced by regional and local geological structures suggesting that the enhanced permeability field in the discharge area enables the formation of the natural thermal springs.

Keywords: thermal spring, conceptual modelling, numerical modelling, recharge area, fractured carbonates, SW Pannonian basin, central Croatia

1. INTRODUCTION

Geothermal systems, which represent a renewable resource for energy and raw material production, vary considerably worldwide due to the different mechanisms governing their formation. They are classified according to their principal properties and characteristics, including their geological, hydrogeological, geochemical, and thermal aspects (MOECK, 2014). A subset of geothermal systems is referred to as hydrothermal when the heat transfer mechanism involves circulating water, whether as liquid or vapour (OJHA et al., 2021; KHODAYAR & BJÖRNSSON, 2024). In the study of hydrothermal systems, it is necessary to determine the origin of the fluid and the area of recharge, the heat transfer mechanism, the direction of fluid flow and the depth to which it descends, the geometry of the aquifer and its hydrogeological and thermal properties, and the conditions favouring the outflow of the thermal water.

Research of hydrothermal systems usually includes the application of an integrated multidisciplinary approach. The geological framework and tectonic evolution of the area influenced by the circulation of thermal fluids are typically recon-

structed by combining regional and local field investigations and geophysical data (e.g., MUFFLER & CATALDI, 1978; FLOVENZ et al., 2012; KOSOVIĆ et al., 2023, 2024). They provide insights into the surface geometry of geological formations and fracture networks and the kinematics of fault systems that are consequently used for subsurface geological reconstructions, supported by 2D or 3D geological modelling. Hydrogeochemical research is the requisite for understanding and managing geothermal aquifers. It involves continuous monitoring of the thermal water to evaluate baseline levels, track their changes, and assess the impact of water abstraction, which is crucial for resource protection and legislative compliance (HOUNSLOW, 1995; MARINI, 2000; MAZOR, 2004; HEASLER, 2009). Analysis of groundwater chemistry and isotopic content aids in characterising hydrothermal systems, identifying water sources, estimating reservoir temperatures, and assessing potential mixing. Hydrogeological research helps in understanding the overall groundwater regime and distribution by providing data (i.e., hydraulic parameters of the aquifer and surrounding rocks, water flow velocities) on sub-

surface conditions influencing the water circulation (FETTER 2001; GOLDSCHIEDER et al. 2010; SZANYI & KOVÁCS, 2010; LEI & ZHU, 2013; RMAN, 2014; FABBRI et al., 2017). Quantifying and monitoring the hydrogeological parameters of the thermal aquifer and water is necessary for predicting the exploitable water volumes with an acceptable drawdown and identifying detrimental effects on the system. Additionally, thermal parametrisation of the geological units involved in the thermal fluid flow helps define the changes in the temperature field and fluid distribution across the system (FUCHS & BALLING, 2016; XIONG et al., 2020).

The investigations mentioned above aid in the construction of a conceptual model of the studied hydrothermal system. Developing the conceptual model of a hydrothermal system consolidates the existing understanding by integrating multidisciplinary and multiscale datasets. Conceptual models describe the main processes governing both fluid flow and heat transport, which influence the volume of the hydrothermal resource and its geochemical and thermal characteristics. The aforementioned geological reconstructions serve as the foundation for a hydrogeological conceptual model of the hydrothermal system, elucidating the mechanisms governing hydrothermal resource formation (MOECK et al., 2014; CALCAGNO et al., 2014, MROCZEK et al., 2016). The physical reliability of the conceptual model can be constrained by developing variable-density fluid flow and heat transport numerical simulations of the system. Numerical models can be used for testing and quantifying the importance of different processes in the development of the geothermal resource and its physicochemical characteristics (e.g., MÁDL-SZÓNYI & TÓTH, 2015; HAVRIL et al., 2016; MONTANARI et al., 2017; BOROVIĆ et al., 2019; POLA et al., 2020; TORRESAN et al., 2022). Furthermore, they can be used to reconstruct the historical and current state of the system and to forecast future impacts (ANDERSON et al., 2015).

Thermal springs in Croatia are generally part of intermediate-scale hydrothermal systems, including recharge areas in the nearby mountainous hinterlands and geothermal aquifers mainly hosted in Mesozoic carbonate rocks (GOLDSCHIEDER et al., 2010; BOROVIĆ et al., 2016). Their occurrence is favoured by the regional thermal characteristics in central and northern Croatia that are part of the Pannonian Basin System (PBS). The tectonic setting of the PBS is characterised by the thinned lithosphere, which enables an above-average heat flow from the asthenosphere (HORVÁTH et al., 2015). In the PBS, three levels of the regional flow of thermal water have been identified: i) gravity flows in the Neogene-Quaternary clastic rocks and sediments of the basin fill (the shallowest), ii) gravity flows in pre-Neogene confined carbonate aquifers below them, and iii) flow caused by overpressure in the deepest Mesozoic aquifers (HORVÁTH et al., 2015; VASS et al., 2018). The Mesozoic carbonate rocks, representing the deepest geothermal aquifers, usually crop out either as inselbergs or along the margins of the basin. This could imply the occurrence of greater recharge in the marginal parts of the PBS, where the aquifer is shallower and covered by thinner Neogene deposits, favouring the development of local to intermediate scale hy-

drothermal systems (STEVANOVIĆ, 2015; HAVRIL et al., 2016).

The artesian thermal springs of Topusko have been renowned since Roman times, ranking as the second warmest in Croatia (BOROVIĆ et al., 2016; ŠIMUNIĆ, 2008). Thermal water with temperatures of up to 65°C has been used since the 1980s for health and recreational purposes and district heating. Despite this fact, the geological features driving the development of the Topusko hydrothermal system (THS) and regulating the regional groundwater flow direction remained uncertain. In the initial stages of THS research, the potential recharge area was determined by defining outcrops of permeable rocks in topographically prominent areas. The lack of previous systematic and detailed structural-geological and hydrogeological investigations hindered the reconstruction of the regional geological evolution and understanding of how the THS functions. Though available publications and unpublished reports suggest contradictory hypotheses, the most commonly used conceptual model is from the early 2000s (ŠIMUNIĆ, 2008). In this study, we propose a novel conceptual model of the THS, detailing the recharge area and main circulation paths using a collection of structural, geochemical, and hydrogeological field data. The second objective of this research involves conducting 2D numerical modelling to analyse fluid flow and heat transport within the THS. Here, the 2D numerical modelling served as a physical validation for the proposed conceptual model, supporting it with the quantification of the main processes governing the development of the Topusko geothermal resource.

2. MATERIALS AND METHODS

2.1. Tectonic setting

The THS formed in the pre-Neogene basement units of the Internal Dinarides (Fig. 1). The Internal Dinarides, as an integral part of the Adria Microplate, convey Adria's eastern passive margin that was involved in a complex tectonic collision between the Adria Microplate and European foreland during the Cretaceous-Paleogene period (SCHMID et al., 2020 with references).

This tectonic contraction (the recent convergence rate between the Adria indenter and Europe is ≤ 4.17 mm/yr according to D'AGOSTINO et al. 2008) resulted in the formation of a Dinaridic orogen system, tectonic suture zone (i.e., Sava Suture Zone), and 400 km eastward extrusion of the ALCAPA block (i.e., Eastern Alps, West Carpathians and Transdanubian ranges; TARI et al., 1999; CSONTOS & VÖRÖS, 2004). Besides the formation of an orogen-parallel thrust fault system, tectonic contraction accommodated the formation of regional dextral/sinistral faults (e.g., the Split-Karlovac fault, Periadriatic fault that extends into the Mid-Hungarian fault zone further to the E; Fig. 1), which enabled CCW/CW rotation and partial tectonic exhumation of the nearby tectonic blocks of the Adria Microplate and the Tisza-Dacia Mega-Unit (e.g. TOMLJENOVIĆ, 2002; TOMLJENOVIĆ et al., 2008; USTASZEWSKI et al., 2010; SCHMID et al., 2020).

At the same time, as the study area is positioned in the immediate vicinity of the transient zone between the Adria



Figure 1. Regional tectonostratigraphic units that surround the study area of the THS (red dashed polygon corresponds to the extent of Fig. 3). Map shows the main regional fault systems that accommodated the tectonic collision of the Adria Microplate and European Foreland during Cretaceous-Paleogene time. The study area is located at the eastern margin of the Adria Microplate, within the Internal Dinarides, close to the Sava Suture Zone (modified after SCHMID et al., 2008; 2020).

Microplate (W) and the Tisza Mega-Unit (E), the inherited fault system is characterised by polyphase tectonic evolution and persistent structural reactivation of the faults (Fig. 2; SCHMID et al., 2008). As a result, the THS bedrock units (Fig. 3) resemble a complex lithostratigraphic mosaic of Palaeozoic-Triassic clastic and carbonate units, that are often seen in tectonic contact with younger Jurassic-Cretaceous ophiolitic mélangé units (SCHMID et al., 2008), and its Paleogene-Neogene cover.

The Neogene-Quaternary tectonic evolution of the study area, on the other hand, was further affected by back-arc type formation of the PBS (ROYDEN & HORVÁTH, 1988; HORVÁTH et al., 2006; CLOETINGH et al., 2006). Formation of the PBS was characterised by repeated Early-Middle

Miocene E-W oriented lithospheric extension (c. 26-11.5 Ma), along the NNW-striking normal listric faults (i.e., the Sava fault; Fig. 2), which was followed by its Late Miocene-Pliocene-Quaternary tectonic inversion due to N – S compression (e.g., PRELOGOVIĆ et al., 1998; TARI et al., 1999; TOMLJENOVIĆ & CSONTOS, 2001; CLOETINGH et al. 2006; SCHMID et al., 2008; BRÜCKL et al., 2010).

In the Croatian part of the PBS, a Neogene-Quaternary sediment succession (Fig. 3) is associated with the dominant NNW-striking Sava, Karlovac and Glina basins and subbasins, which were tectonically inverted and highly deformed during the Late Miocene-Pliocene-Quaternary periods (PAVELIĆ, 2001; PAVELIĆ et al., 2003; TOMLJENOVIĆ & CSONTOS, 2001). Tectonic deformation of the Neogene-Quaternary

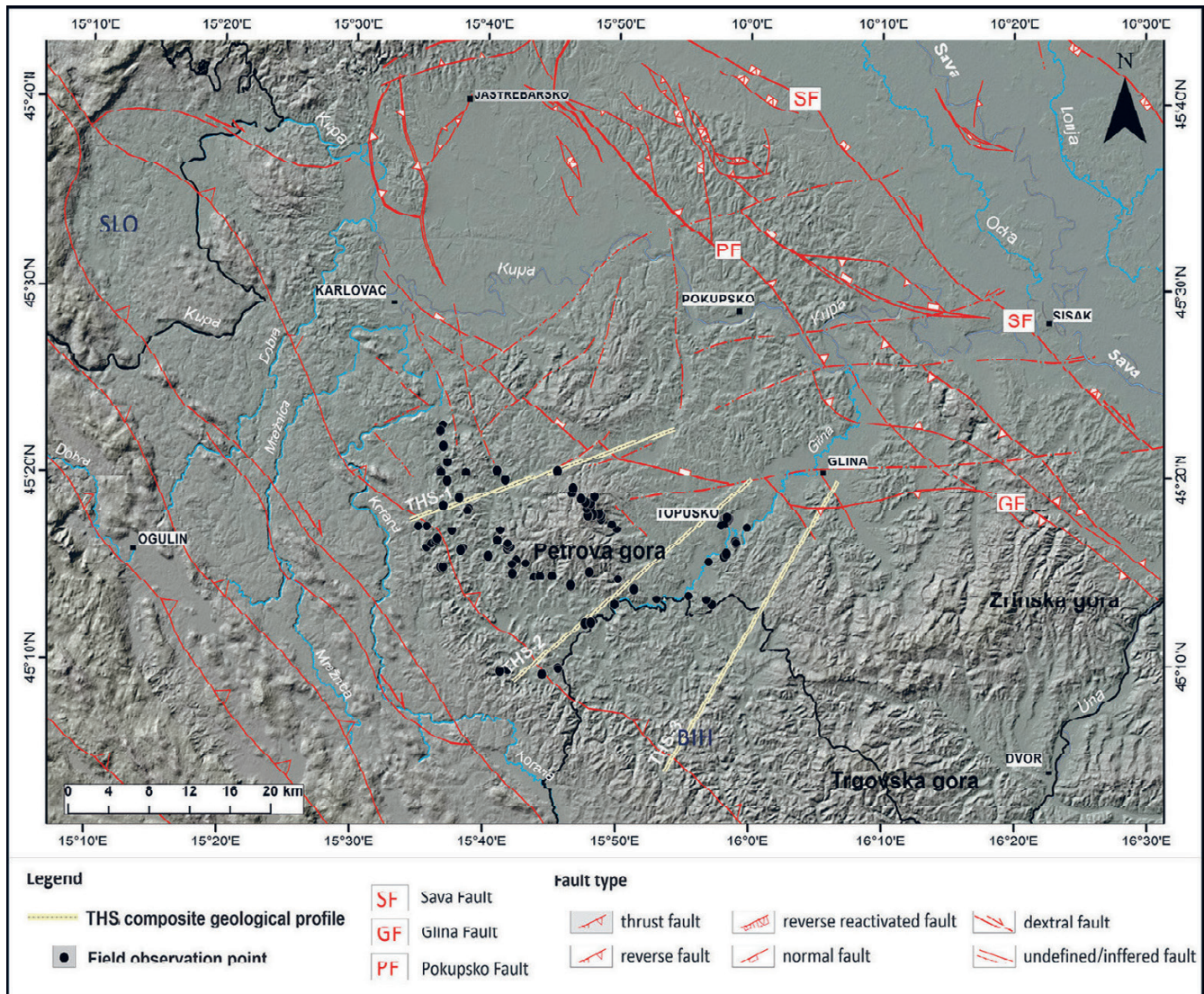


Figure 2. The structural map shows a simplified tectonic framework of the fault systems at the SW margin of the PBS. Fault abbreviations: SF – Sava fault; PF- Pokupsko fault; GF – Glina fault. Fault systems are compiled after KOROLIJA et al. (1980), VELIĆ & SOKAČ (1982), BUKOVAC et al. (1984), PIKIJA (1987), ŠIKIĆ (1990), PRELOGOVIĆ et al. (1998), TOMLJENOVIĆ & CSONTOS (2001), BENČEK et al. (2014), and HERAK & HERAK (2023).

succession in the study area is especially pronounced along the contact with the Palaeozoic-Triassic anticlinal core of the Petrova gora Mt. (HORVÁTH & TARI 1999; TOMLJENOVIĆ & CSONTOS, 2001).

Though tectonic uplift of the Petrova gora Mt. had probably already started during the Cretaceous-Paleogene contraction (similar to the other PBS pre-Neogene basement highs e.g., Trgovska gora, Slavonian Mts.), the final uplift commenced during the Late Miocene-Pliocene-Quaternary compression/transpression phase that resulted in tectonic exhumation, tectonic overprint of its Palaeozoic-Mesozoic structures, and formation of kilometre-scale folds along the reactivated and newly formed faults in the area (Fig. 2; PRELOGOVIĆ et al., 1998; TOMLJENOVIĆ & CSONTOS, 2001). Ongoing, local NNE-SSW regional compression in the study area is driven by residual Adria indentation shortening locally at the scale of 1-2 mm/yr and is accommodated along the inherited faults with slip rates below 0.1 mm/yr (GRENERCZY et al., 2005; KASTELIĆ & CARAFA, 2012; USTASZEWSKI et al., 2014).

2.2. Geological setting

A composite geological map covering the study area (Fig. 3) was constructed using basic geological maps of the former Yugoslavia at a scale of 1:100.000, sheets Karlovac (BENČEK et al., 2014), Sisak (PIKIJA, 1987), Slunj (KOROLIJA et al., 1980), and Bosanski Novi (ŠIKIĆ, 1990), as well as the 1:500.000 scale geological map (FEDERAL GEOLOGICAL SURVEY, 1970). A description of the subsurface geological composition was compiled, including a composite geological column that outlines the lithostratigraphic and chronostratigraphic sequence of deposits in the area. The synthesis of existing data was undertaken using GIS and graphical editing tools.

The geological setting of the study area predominantly comprises Late Palaeozoic, Triassic, and Plio-Quaternary to Quaternary deposits, which cover older Variscan bedrock and structures. In the SE part, Carboniferous deposits (C) are the oldest exposed rocks (Fig. 3). They are predominantly composed of clastic and subordinately carbonate deposits, includ-

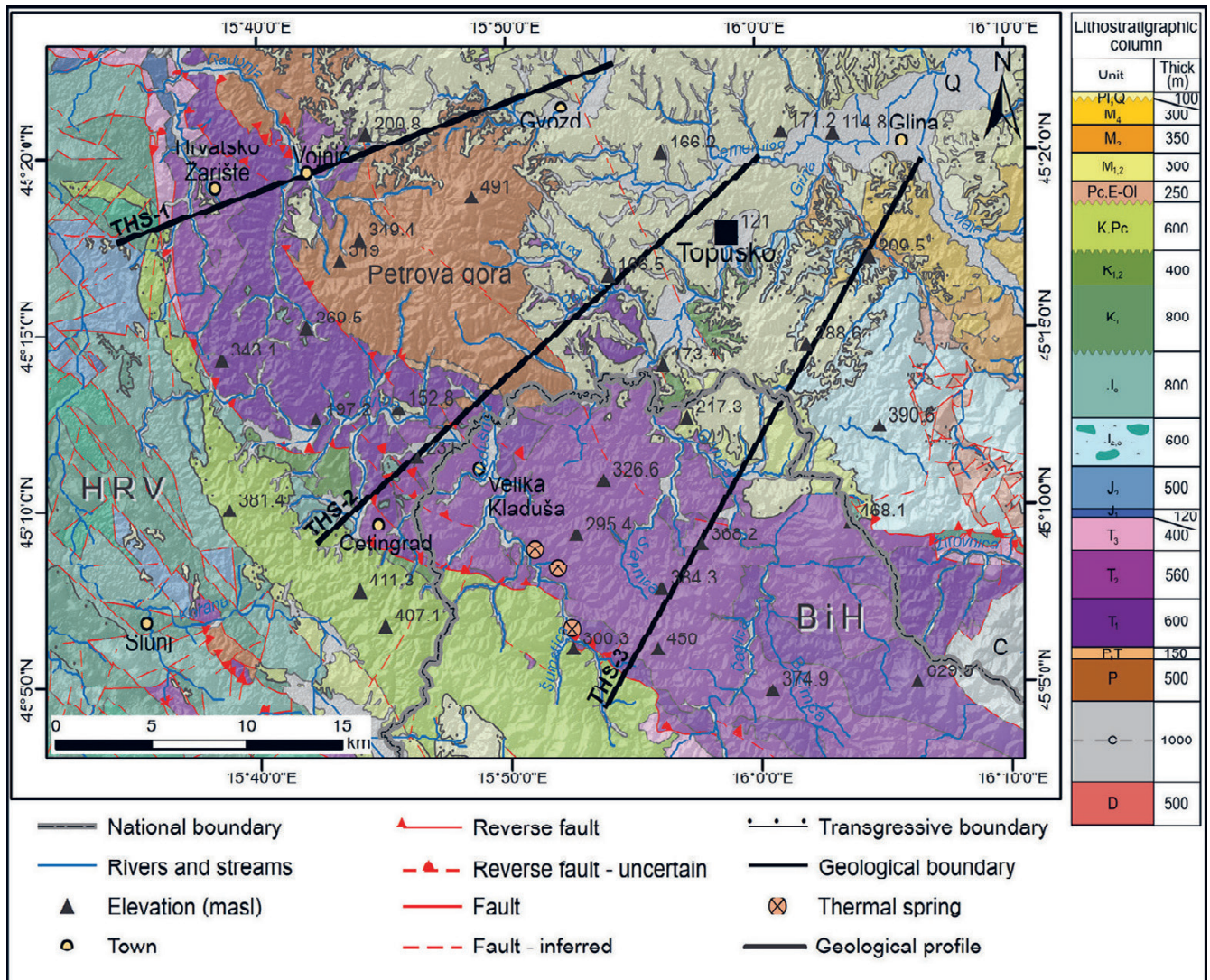


Figure 3. Geological map of the study area of the THS according to the basic geological maps of the SFRY at a scale of 1:100,000, sheets Karlovac (BENČEK et al., 2014), Sisak (PIKJIA, 1987), Slunj (KOROLIJA et al., 1980), Bosanski Novi (ŠIKIĆ, 1988) and geological maps of SFR Yugoslavia, scale 1:500,000 (FEDERAL GEOLOGICAL SURVEY, 1970). Acronyms of the lithostratigraphic units: Q – Quaternary; Pl, Pli, Q – Pliocene, Plio – Quaternary; M – Miocene; Pc, E-Ol – Paleocene and Eocene-Oligocene; K, Pc – Cretaceous-Paleogene K – Cretaceous; J – Jurassic; T – Triassic; P, T – Permian - Triassic; P – Permian; C – Carboniferous; D – Devonian. Thermal springs’ locations in Bosnia and Herzegovina after HRVATOVIĆ (2005). The extent of the study area is shown in Figure 1.

ing shales, siltites, sandstones (greywacke, quartz-greywacke), and dolomitised and ankeritised limestones. Together with the Devonian deposits (D), characterised by thick lenses of clay, limonitised and schistose limestones within interbeds of shales, siltstone and sandstones form the pre-Permian low-grade metamorphic basement (ŠIKIĆ, 1990).

Continuation of the post-Carboniferous deposition sequence is characterised by a clastic sequence of younger Palaeozoic age and is found on the southern slopes of Petrova gora Mt. (Fig. 3). Permian deposits (P) are represented by schists, quartz-greywacke sandstones, shales, and fine-grained conglomerates (KOROLIJA et al., 1980). This turbidite-like complex was developed under conditions of rapid and constant infilling within the existing basement basinal structures, reaching thicknesses of 500 m. At the same time, Permo-Triassic deposits (P, T) are consistent and composed of fine-grained brick-red sandstones and sandy-clay shales (KOROLIJA et al., 1981). The quartz-rich greywackes of the Upper Permian, observed along the southern slopes of the Petrova

gora Mt., are a marker that represents transitional strata from the Upper Permian to the Lower Triassic (Fig. 3), which were deposited in shallower marine environments due to orogenic uplift.

Lower Triassic (T₁) deposition of mica sandstones, siltites, and shales with a gradual transition to carbonate marls and eventually limestones and dolomites continuously followed the Upper Palaeozoic normal superposition (KOROLIJA, 1981). These deposits can be observed on the eastern slopes of Petrova gora Mt., concordantly overlapping older Permian deposits (Fig. 3). During the Middle Triassic (T₂), evidence of consistent limestone and dolomite deposition can be observed. At the local scale, within the carbonate facies, tuffs, fine-grained sandstones, and interlayers of sheet limestone with chert alongside the shales were observed. The diminishing presence of clastic and pyroclastic components within the uppermost Middle Triassic succession suggests a reduction in tectonic activity and volcanism. During the Late Triassic period (T₃), stable marine conditions enabled further massive

carbonate deposition in the area. The Upper Triassic dolomites (W of Hrvatsko Žarište, Fig. 3) are usually in tectonic contact with the Lower – Upper Cretaceous limestones.

According to SCHMID et al. (2008), Late Jurassic regional movements prompted the intraoceanic subduction of the Neotethys oceanic realm, which coexisted with the fragmentation of the Adria Microplate. This led to the Adria Microplate terrain differentiation, which resulted in variable sedimentation patterns and continuous Jurassic-Cretaceous carbonate sedimentation in the area of the Adriatic Carbonate Platform (VLAHOVIĆ et al., 2005), while clastic-carbonate-volcanic sedimentation prevailed along its passive margins. The Jurassic rock complex in the study area (J_{2,3}), part of this passive margin, primarily comprises a magmatic-sedimentary ophiolitic complex within the Central Dinaridic Ophiolitic Zone (SCHMID et al., 2008). This approximately 800 m thick complex consists of low-metamorphosed sedimentary rocks, (i.e., sandstones, shales, cherts, and some siltites, marly shales, and fine-grained limestones) and various magmatic rocks (i.e., basalts, gabbros, diabases; KOROLIJA et al., 1981; ŠIKIĆ, 1990).

The Cretaceous-Paleogene transgressive sequence (Fig. 3) indicates passive margin sedimentation (KOROLIJA et al., 1981). Cretaceous deposits (K₁) include limestones, greenish-gray marls, silicified sandstones, and carbonate breccias, followed by a flysch-turbidite like succession (K_{1,2}) (VLAHOVIĆ et al., 2005). Paleogene deposits are mainly flysch-like, with carbonate marls, marly limestones, and thin layers of shales, marls, and fine-grained sandstones (K, Pc). Palaeocene and Eocene-Oligocene flysch-like deposits (Pc, E-Ol) crop out to a small extent in the eastern part of the study area. The Neogene-Quaternary sediment succession, linked to the tectonic evolution of the Croatian part of the PBS, was deposited in half-graben structures formed during the Early-Middle Miocene (PRELOGOVIĆ et al., 1998; TOMLJENOVIĆ & CSONTOS, 2001; SAFTIĆ et al., 2003). Extensional tectonics led to basins filled with marine, lacustrine, and freshwater sediments (PAVELIĆ et al., 2003). This succession, about 1.1 km thick, includes conglomerates, sandstones, gravels, clays, marls, and limestones (M; Pl, Q; Fig. 3) (ŠIKIĆ, 1990). The youngest Pliocene and Quaternary deposits (Pl; Q), approximately 200 m thick, consist of conglomerates, sandstones, siltstones, sands, gravels, clays, and occasional interlayers of clay and coal, forming a final terrigenous/alluvial cover.

2.3. Hydrogeological setting

In the Topusko area, there are three natural artesian thermal springs with a total capacity of approx. 25 l/s (BAĆ & HERAK, 1962; BAHUN & RALJEVIĆ, 1969) and temperatures ranging from 46 °C to 53 °C. Three exploitation wells were drilled to depths of up to 250 m in the immediate vicinity of the natural springs during the 1980s. They are currently used for heating, recreational, and medicinal purposes, with a total yield of 200 l/s and pressure of around 1.4 bar (PAVIĆ et al., 2023). A decrease in pressure from 2.18 bar (1978) to 1.52 bar (1982) was observed and attributed to overexploitation (ŠEGOTIĆ & ŠMIT, 2007). The Topusko thermal water shows a slightly acidic character, with an average pH of 6.5 – 6.8. The

electrical conductivity ranges from 582 μS/cm to 680 μS/cm, and the total dissolved solids are approx. 500 mg/l indicating a medium to low mineralised fresh water. Hydrochemical analyses show a Ca-HCO₃ hydrochemical facies (PAVIĆ et al., 2023, 2024) indicating water flow in carbonate rocks. Stable water isotopes δ²H and δ¹⁸O suggest a meteoric origin for thermal water and recharge during colder climatic conditions. The uniform δ¹⁸O values indicate deep circulation and a large, thick aquifer, which homogenises seasonal precipitation variations over longer residence times. The estimated mean residence time of approximately 8.5 – 9.5 kyr is based on ¹⁴C content in DIC (PAVIĆ et al., 2024). Tritium activity in the thermal water is generally below the detection limit, but trace levels were detected after extensive abstraction for district heating during winter months, suggesting the potential infiltration of modern precipitation through the semi-permeable Neogene cover sequence of the aquifer. The most plausible equilibrium aquifer temperature was estimated at 90 °C using quartz geothermometers (PAVIĆ et al., 2023, 2024). Hydrodynamic measurements in the Topusko discharge area estimated an aquifer transmissivity of approx. 2 x 10⁻² m²/s (PAVIĆ et al., 2023). According to ŠIMUNIĆ (2008), a set of faults forming a block in the shape of a three-sided prism enabled the uplifting of the aquifer. The result of an electrical resistivity survey identified the damaged zones of these faults in the spring area (PAVIĆ et al., 2023).

From a hydrogeological point of view, fractured and karstified, highly permeable, Middle and Upper Triassic carbonates are the main geothermal aquifer of the THS. Lower Triassic and Permian-Triassic carbonate and clastic rocks represent the semi-confining units at the base of the reservoir, while the Palaeozoic complex is the impervious basement at the bottom of the stratigraphic sequence due to its low-grade metamorphism. Furthermore, low permeability Jurassic ophiolitic complex and Neogene-Quaternary deposits cover the geothermal aquifer. However, a limited number of deep boreholes hinders a more comprehensive understanding of local and regional scale hydrogeological conditions.

Different conceptual models of the THS have been previously proposed:

1) In the early 20th century, it was considered that the thermal water at the Topusko springs was heated by a magmatic body based on the existence of basalt outcrops in the vicinity (e.g., Lasinja GORJANOVIĆ-KRAMBERGER, 1905, 1917). To support the volcanic origin of the thermal water in Topusko, GORJANOVIĆ-KRAMBERGER (1917) postulated that mountains S of Topusko could not produce such hydrostatic pressure that would raise water from a depth of approx. 1.5 km, according to the thermal water temperature at the surface. However, these basalts are of Mesozoic age (MAJER, 1978; 1993) and Quaternary magmatic bodies behaving as a recent heat source for hydrothermal systems are absent within the PBS. Therefore, this conceptual model was abandoned.

2) BAĆ & HERAK (1962) interpreted the Palaeozoic rocks as behaving as an impermeable rock complex that regulates regional water circulation and defines the watershed of the THS together with Lower Triassic and Neogene formations. According to the same authors, permeable Middle

and Upper Triassic carbonate deposits facilitate deep groundwater circulation, especially in tectonically active areas. The thermal aquifer receives recharge in the Glina river headwaters, where Triassic carbonates crop out. The proposed primary regional flow direction is from the S to N, from the Glina area towards the Topusko depression.

3) ŠIMUNIĆ (2008) proposed that the THS recharge area is located W of the Petrova gora Mt., where Triassic carbonates crop out. According to the proposed model, the water circulates from W to E below the Petrova gora nappe, heats up by the geothermal gradient, and discharges in Topusko due to the highly permeable fault damaged zones.

2.4. Structural-geological research

Structural-geological fieldwork was conducted through field campaigns in 2021 and 2022. Field investigations involved structural and lithological data acquisition at 162 locations covering an area of approx. 2,000 km² (Figs. 2 and 3). During the fieldwork, observation points were archived and processed in the Avenza PDF Maps application (URL 1) and MS Excel field database, while database creation and geospatial positioning of the collected geological data were performed using the software ArcMap 10.1 (URL 2).

The structural investigations detailed the stratigraphic relationships among the main lithological units and the analysis of the tectonic and structural settings in the study area. They encompassed geometric and structural measurements of strata bedding, fractures/joint systems, and fault/shear planes. In particular, measurements of fault/shear planes included the identification of fault kinematic indicators and determination of the tectonic relationships between the observed structures. Collected structural data were used in the construction of three NE-SW striking regional structural-geological profiles (THS-1 to THS-3; Figs. 2–4). These profiles represent surface/sub-surface 2D models of the distribution of geological units and structures in the area of Petrova gora Mt. (SW) and the Glina depression (NE) and they were used here for reconstruction of the geological and structural settings of the THS.

2.5. Conceptual and numerical modelling

In this study, we initially tested and compared the validity of the conceptual model proposed by ŠIMUNIĆ (2008) with the results of structural investigations and the constructed geological profiles. Furthermore, these data combined with the results of previous investigations in the Topusko area were used to update the conceptual model of the THS, which served as a base for a 2D numerical model of heat flow and fluid transport. The conceptual model was developed including: lithological field data, geological maps, hydrodynamic and electrical resistivity survey data acquired in the discharge area of Topusko, chemical and isotopic compositions of both the thermal water and the precipitation in the assumed recharge area.

The proposed conceptual model was tested by performing numerical simulations of fluid flow and heat transport accounting for the variation of the thermal water density due to the temperature distribution in the subsurface (BUNDSCHUH & ČEŠAR SUÁREZ, 2010; DIERSCH, 2014).

The numerical model solves the governing equations of fluid flow and heat transport, obtaining the distribution of the primary variables (i.e., hydraulic head and temperature) within the modelling domain and over time. In this research, we used the FEFLOW 7.4 software (DIERSCH, 2014), a Finite Element-based simulator specifically designed to address fluid flow and transport phenomena within porous and fractured media. The fundamental equations governing fluid flow and heat transport in these media are formulated based on conservation principles for fluid mass, momentum, and thermal energy (DIERSCH, 2014). The equations are coupled by setting a functional form behaviour for fluid density and viscosity depending on the respective primary variable of the problem. For the specific problem at hand, fluid viscosity was kept constant. In contrast, the density of the fluid varies linearly with temperature, following $\rho = \rho_0(1 - \alpha\Delta T)$ with α being the volumetric thermal expansion coefficient of the fluid (POLA et al., 2020).

3. RESULTS

3.1. Structural-geological profiles

Structural – geological profiles THS-1 to THS-3 (Fig. 4) represent an interpretation of the surface/subsurface relationships in the study area down to an investigation depth of approx. 6 km. Constructed geological profiles include three structural domains that convey a system of thrust faults separating the External Dinaridic lithological units in the SW parts of the profiles from the Internal Dinaridic lithological units. The Internal Dinaridic units can be further subdivided into two subdomains. The SE and central part of the profiles included the Petrova gora area, while the Glina depression characterises the NE profile domains (Fig. 4).

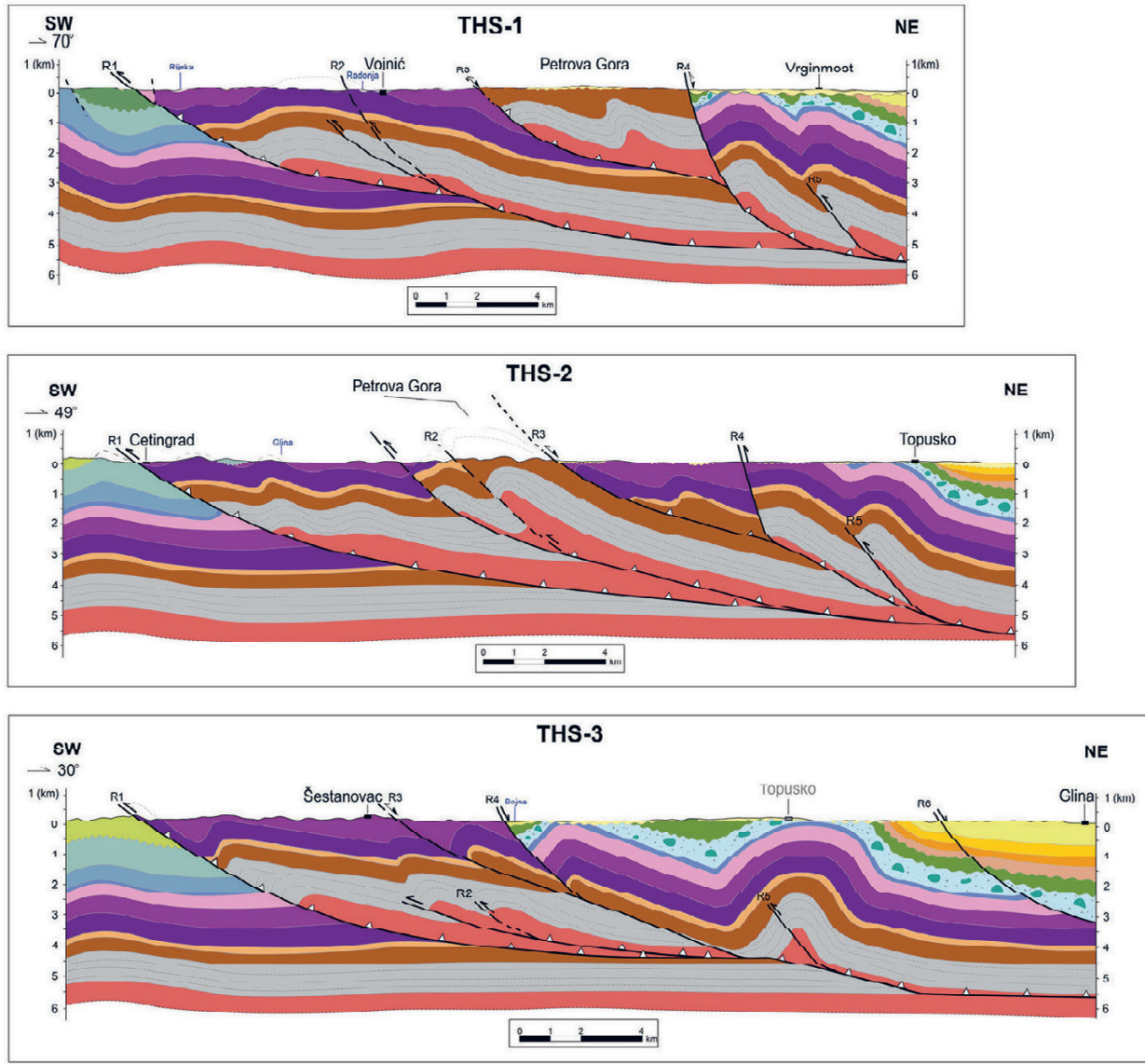
The profiles (Figs. 2 and 4) pinpoint complex faulted and folded structures that are predominantly affected by low angle thrust faults (dip angle $\leq 30^\circ$; faults R1, R2, and R3 in Fig. 4) and reverse faults in their immediate hanging wall (faults R5 and R2 in Fig. 4). Besides these faults, higher angle normal and tectonically inverted normal faults are observed (dip angle $\geq 45^\circ$; faults R4 and R6 in Fig. 4). Constructed profiles show that the THS subsurface is composed of folded structures, with the largest Topusko anticline formed in the hanging wall of the R3 thrust fault and R5 blind fault (profile THS-3 in Fig. 4). The Petrova gora structure also resembles a larger-scale anticlinal structure that is tectonically uplifted in the hanging walls of the R1 and R2 thrust faults (profile THS-1 in Fig. 4).

The Petrova gora structure, composed of a Palaeozoic clastic sequence, is tectonically uplifted by approx. 3.5 km in relation to its R1 footwall units, which resemble an undeformed, 6 km thick, Palaeozoic-Mesozoic succession. Towards the NE, the Petrova gora structure is additionally vertically displaced by tectonically inverted normal faults (faults R3 and R4; profile THS-1 in Fig. 4). Here, vertical displacement along the R3 and R4 normal faults accommodates NE-SW oriented extension, with approx. 1.5 – 2 km vertical subsidence.

Further to the NE, the R4 fault delineates a folded system that incorporates the area of the Topusko anticline. With an approx. 4 km thick Palaeozoic-Mesozoic succession, this folded system (profile THS-3 in Fig. 4) is mainly composed of the Carboniferous-Permian clastic succession that is covered

by Triassic clastic-carbonate rocks. The Topusko anticline hinge zone is partly covered by the Jurassic ophiolitic complex and its transgressive Cretaceous clastic-carbonate succession

(see Figs. 3 and 4, profile THS-3). In the area of the Topusko anticline, both the Cretaceous and Jurassic units are significantly reduced due to extensive uplift along the R5 blind



LEGEND

Quaternary Recent river alluvial deposits	Late Cretaceous-Paleocene Flysch deposits: sandstone, marls, limestone lenses	Late Triassic Interchange of early-late diagenetic dolomite and limestone	Devonian Shistic shale, sandstone and intercalations of limestone	Transgressive boundary
Pliocene-Quaternary Gravel and sands	Late Cretaceous Flysch deposits: marls, silica rich sandstone, calcarenite, carbonate breccia	Middle Triassic Dolomite limestone shale, cherts, tuffs and sandstone		Thrust sheet
Late Miocene Gravel, silt, clay, marls & fossiliferous limestone, coal, pyroclastite	Early Cretaceous Limestone with dolomite intercalations	Early Triassic Limestone, dolomite, sandstone, marls, shale		Reverse fault
Middle Miocene Limestone, gravel, sand, sandstone, marl	Late Jurassic Dolomites, dolomitized limestone	Permian-Triassic Quartz-rich sandstone, silt, conglomerate, slate		Normal fault
Early Miocene Sandstone, marls, limestone	Late-Middle Jurassic Ophiolitic mélange unit, basalt, gabbro, shale, radiolarite, limestone	Permian Siltstns, sandstone and conglomerate		Normal fault - tectonically inverted reverse fault
Paleogene-Oligocene Conglomerate, breccia, sandstone, marls, limestone, chalo, siltite, coal	Early Jurassic Laminated dolomite with lenses of limestone	Carboniferous Sandstone, shale, conglomerate, dolomite and fossiliferous limestone		Inferred fault

Figure 4. Structural-geological profiles in the THS area. The NE-SW striking profiles are perpendicular to the geological structures in the research area. The profiles show the Topusko anticline formed in the hanging wall of the thrust fault R3 that behaves as a low-angle detachment surface. The anticline is composed of a thick Palaeozoic-Mesozoic sequence, which is partly eroded in the immediate area of Topusko town. Towards the NE, it is covered by the thick Paleogene-Neogene sedimentary succession of the Glina depression. Horizontal and vertical scale ratio is 1:1.

fault, which resulted in hanging wall tectonic erosion. The final NE domains of the THS geological profiles incorporate the gently dipping NE limb of the Topusko anticline that is faulted by the NE dipping R6 normal fault. The R6 normal fault (vertical displacement here is approx. 500 m; profile THS-3 in Fig. 4) is part of the extensional structure of the Glina depression, which is one of the extensional basins formed during the Neogene extension of the Croatian part of the PBS. As a result, the NE segments of the THS profiles are covered by an additional approx. 2 km thick clastic-carbonate succession deposited during the Paleogene and Neogene within the Glina depression.

Reconstructed THS subsurface relationships along the profiles indicate that the observed faults and cogenetic folded structures have a history of polyphase deformation. The same asymmetric anticlinal structures (e.g., Petrova gora) in the hanging wall of the low angle detachment faults (e.g., R3 and

R4 faults, Fig. 4) show indications of tectonic transport towards the SW, localised uplift and erosion (e.g., Topusko anticline), as well as NE – SW oriented extension. This implies that the interpreted faults accommodated both initial Cretaceous-Paleogene NE – SW compression and the following Neogene NE – SW extension.

3.2. Conceptual and numerical modelling of groundwater flow and heat transport in the THS

3.2.1. Novel conceptual model of the THS

The new conceptual model of the THS is established based on constructed geological profiles (Fig. 4) and previous hydrogeological and geophysical research (PAVIĆ et al., 2023, 2024). These data lead to development of an interpolated schematic geological profile, which refines the understanding of the THS (Figs. 5 & 6). Analysis of the geological profiles

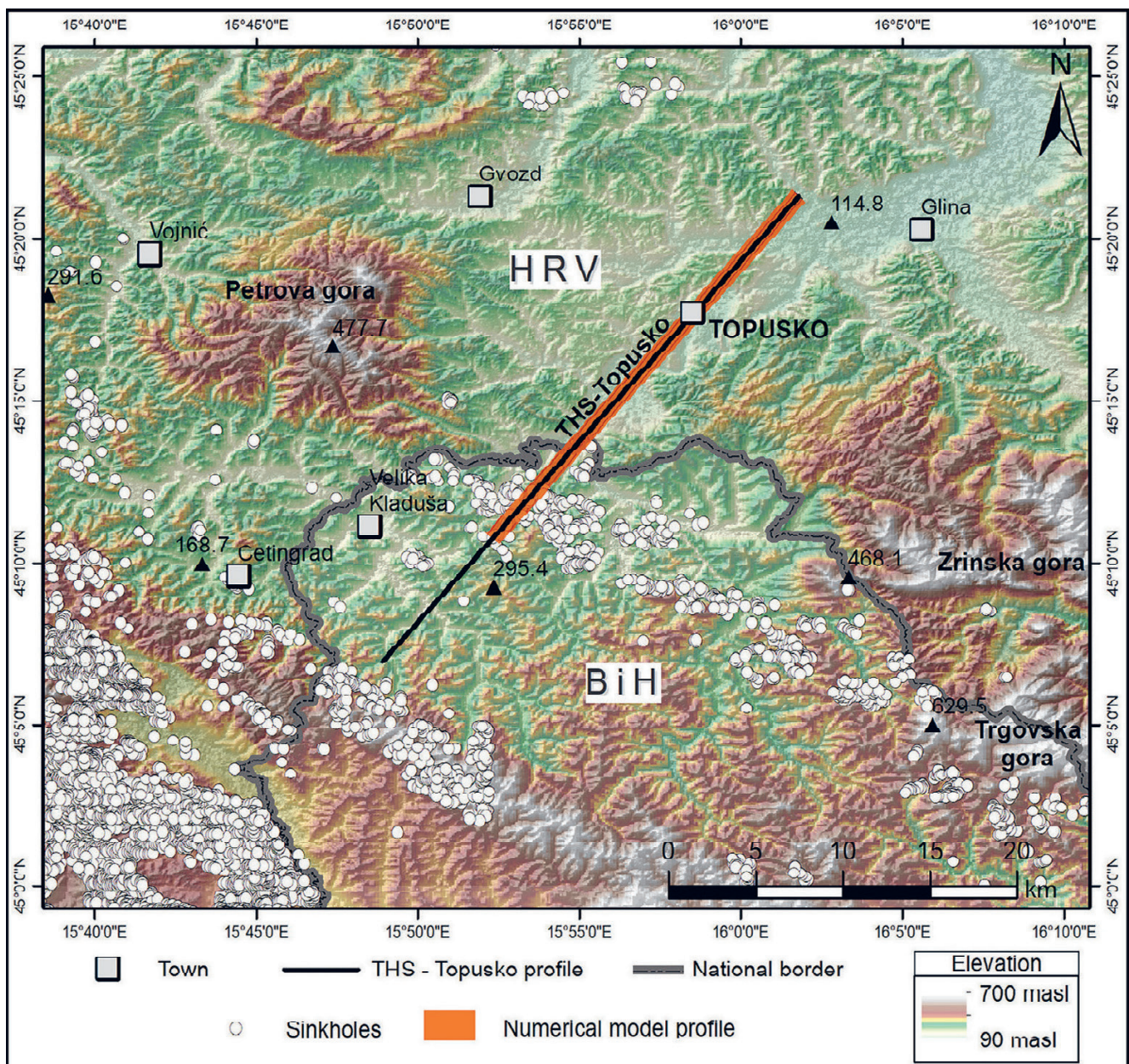


Figure 5 Trace of the interpolated schematic geological profile of the THS (black line). Sinkholes (white circles) in the SW part of the profile indicate higher karstification of the carbonate formations, representing the potential recharge area of the THS.

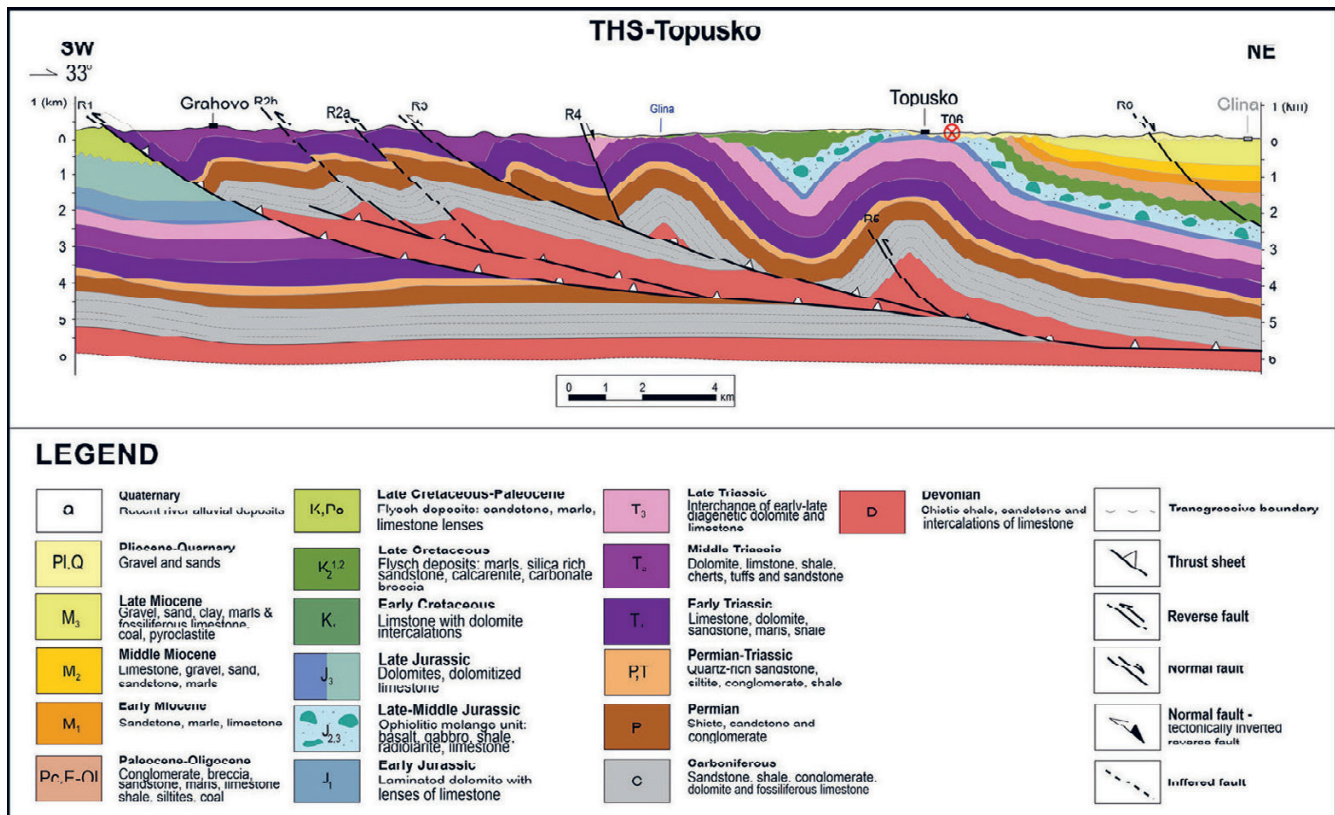


Figure 6. Interpolated geological profile of the THS. The profile is perpendicular to the Topusko anticline formed in the hanging wall of the thrust fault R3 that behaves as a low angle detachment surface. The same fault, combined with the R4 and R5 reverse faults, lifts the reservoir up to shallow depths in the immediate area of Topusko town. Horizontal and vertical scale is 1:1.

here, challenges the previously proposed hypothesis by ŠIMUNIĆ (2008) about the recharge area of the THS being W of the Petrova gora nappe. The Triassic carbonates cropping out W of the Petrova gora Mt. are hydrogeologically isolated from the discharge area in Topusko by the impermeable Petrova gora structure, which is composed of a Palaeozoic clastic sequence with low-grade metamorphism. Therefore, a regional groundwater flow from W to E becomes highly unlikely. Instead, in our conceptual model, attention is directed towards a new hypothesis: the recharge occurs S from Topusko, where Triassic carbonates are partly exposed at the surface.

The surface manifestation of thermal water in the Topusko spring area can be understood through the concept of gravity-driven groundwater flow, determined by: i) Middle-Upper Triassic carbonate complex rocks, which are the main thermal aquifer of the THS, ii) Palaeozoic-Lower Triassic and the Jurassic-Neogene formations representing the semi-confining layers at the bottom and top of the reservoir, respectively, iii) a large area characterised by intense karstification occurring approx. 13 km S of Topusko within the Triassic carbonates (Fig. 5), facilitating the infiltration and deep circulation of the meteoric water with a long residence time, and iv) the fault-thrusted regional tectonic setting and the existence of substantial hydraulic boundaries (e.g., the R3 and R4 thrust faults and near-surface fault zones), which influence the direction of the groundwater flow. The Topusko anticline within the hanging wall of the R3 thrust fault facilitates the uplift of the aquifer, bringing it closer to the surface in the thermal springs area. Cogenetic faults and fracture networks

in the hinge zone of the Topusko anticline, probably affected by an extensional regime, increase the fracturing of the bedrock and the permeability field in the aquifer enabling the thermal water outflow. The occurrence of fault damage zones in the Topusko subsurface was determined by the electrical resistivity surveys (PAVIĆ et al., 2023). Hydrogeochemical research corroborates the meteoric origin of the Topusko thermal water and the interaction with the carbonate aquifer. A residence time of approx. 9 kyr is evidenced by the ¹⁴C analysis of the thermal water (PAVIĆ et al., 2024). Additionally, the consistent major ion composition of the thermal water over a two-year period suggests a large and stable system. Based on all findings, it is suggested that the novel THS conceptual model favours a regional groundwater flow direction from S to N.

3.2.2. Setup of the numerical model

The physical validity of the proposed conceptual model of the THS was tested by conducting 2D numerical modelling of both the regional fluid flow and heat transport. To simulate gravity-driven groundwater flow in the THS, we adopted a shortened version of the schematic geological profile (Fig. 6), excluding the SW portion of the R3 fault. The recharge area of the THS is located NE of R3, where numerous sinkholes occur (Fig. 5). Therefore, the SW portion of the section is not strictly connected to the hydrothermal system, and was not reproduced in the numerical model to diminish the computational effort for solving the numerical simulations. The profile was digitised in GIS software and used to generate a su-

permesh in the FEFLOW software outlining the geometry of the geological units within the modelling domain. The domain was discretised through a triangular mesh employing the Triangle triangulation code (DIERSCH, 2014), which permits honouring the complex geometrical relationships of the units. The mesh was refined in the hinge zone of the Topusko anticline, in the aquifer unit, and along the main faults. Such refinement allows a better discretisation in the parts of the model where numerical instability is expected. The obtained mesh (Fig. 7) comprised 19,241 triangular elements and 9,831 nodes.

Geological units with similar hydrogeological and thermal properties were grouped, obtaining seven hydrostratigraphic units: i) Palaeozoic low-metamorphic sedimentary complex (B), ii) Permian and Permian-Triassic clastic units (P), iii) Early Triassic sedimentary rocks (T_1), iv) Middle and Late Triassic carbonates ($T_{2,3}$), v) Jurassic magmatic – sedimentary ophiolitic complex and Jurassic and Cretaceous carbonates (J), vi) Neogene siliciclastic units (N), and vii) Quaternary alluvial cover (Q). In particular, the $T_{2,3}$ hydrostratigraphic unit represents the main thermal aquifer of the THS. The equivalent porous medium approach was employed for the hydrogeological and thermal parametrisations of the hydrostratigraphic units (DIERSCH, 2014; ANDERSON et al., 2015). This approach considers the unit as a porous medium with homogeneous and isotropic properties being suitable for the numerical modelling of regional groundwater flow systems in heavily fractured and karstified carbonate rocks (TEUTSCH & SAUTER, 1991; SCANLON et al., 2003; GHASEMIZADEH et al., 2012; MÁDL-SZŐNYI & TÓTH, 2015). In a regional numerical model, the scale of these discontinuities is smaller than the representative elementary volume (i.e., the mesh size), resulting in a constant and homogeneous value of the considered parameter. For assigning the hydraulic and thermal properties (Table 1), we considered the main lithology of the hydrostratigraphic units and relied on data from the literature (CERMAK & RYBACH, 1982; DOMENICO & SCHWARTZ, 1997; FETTER, 2001; STYLIANOU et al., 2016; BOROVIĆ et al., 2018; STÖBER & BUCHER, 2021; LALOUÏ & ROTTA LORIA, 2020), parametrisation of similar units in hydrothermal systems within the PBS (RMAN & TÓTH, 2011; MÁDL-SZŐNYI & TÓTH, 2015; HAVRIL et al., 2016), and datasets obtained from field investigations in Topusko (PAVIĆ et al., 2023). The hydraulic conductivity (K) and the porosity (ϕ) were assigned accounting for the role of the units in the THS. Excluding the loose sediments of the Quaternary cover (Q unit; Fig. 3), the highest K and ϕ values were assigned to the $T_{2,3}$ hydrostratigraphic unit representing the thermal aquifer. Conversely, the impervious basement B was reproduced using the lowest K and ϕ values. In the hinge zone of the Topusko anticline, K and ϕ were increased simulating the impact of the local scale fracturing that favours the upwelling of the thermal water. Open fractures can increase the permeability and porosity fields enhancing the fluid flow in the aquifer (i.e., FAULKNER et al., 2010; WORTHINGTON et al., 2019; POURASKARPARAST et al., 2024). The regional values of K and ϕ were increased by: i) two orders of magnitude and 10%, respectively, for the $T_{2,3}$, T_1 , and P units, and ii) one order of magnitude and 5%, respectively, for the B unit considering the decrease of fracture apertures with depth. In particu-

lar, the K value of the $T_{2,3}$ unit in the hinge zone of the Topusko anticline was calculated from a collection of transmissivity values obtained from well tests conducted in Topusko (PAVIĆ et al., 2023). Furthermore, the thermal conductivities (λ) of the N and $T_{2,3}$ units were derived from RMAN & TÓTH (2011), MÁDL-SZŐNYI & TÓTH (2015), and HAVRIL et al. (2016), who investigated regional groundwater flow and heat transport patterns in the PBS.

Boundary conditions (BCs) for fluid flow and heat transport were applied at the border of the modelling domain following the conceptual model of the THS. The fluid flow BCs (Fig. 7A) included: i) a 2nd kind (Neumann) BC at the SW part of the top domain, and ii) a 3rd kind (Cauchy) BC at the top of the domain in the Topusko area. The Neumann BC produces an inflow in the modelling domain and was employed to simulate the recharge of the THS. The condition spanned for a length of 2 km, which corresponds to the extension of the area with a higher density of sinkholes along the modelling domain. An inflow of 90 mm/yr was imposed considering an effective infiltration of 10 % (as being used for the simulation of similar hydrothermal systems in a carbonate reservoir in Croatia; BOROVIĆ et al., 2019) and an average annual precipitation of 900 mm (DHMZ, 2021; MARTINSEN et al., 2022). The Cauchy BC simulates a fluid flux through the model boundary depending on: i) the difference between the hydraulic head imposed at the boundary and the value calculated within the domain, and ii) a transfer-rate coefficient (DIERSCH, 2014). Since it is generally used to simulate the variable outflow in springs (ANDERSON et al., 2015), it was employed in the THS numerical model to reproduce the occurrence of thermal springs in the Topusko area. The imposed hydraulic head was set as the average ground elevation (122 masl), while the transfer rate was calculated as the K of the Q unit (Table 1) divided by the thickness of the alluvial cover in Topusko obtained from the stratigraphic well logs. The heat transport BCs (Fig. 7B) included: i) a 1st kind (Dirichlet) BC at the SW and NE vertical boundaries of the modelling domain and at the top except for the Topusko area, ii) a 2nd kind (Neumann) BC at the bottom, and iii) a 3rd kind (Cauchy) BC at the top of the domain in the Topusko area. The Dirichlet BC imposes a constant value of the primary variable. In the THS model, it was used to reproduce both the ground temperature at the surface and the increasing temperature with depth due to the regional geothermal gradient at the vertical boundaries. The temperature imposed at the top was set to 10 °C, which corresponds to the mean average annual air temperature, while the values at the lateral boundary were obtained from the initial distribution of temperature. The Neumann BC was used to simulate the regional inflow of heat from the deeper parts of the crust. A value of 100 mW/m² was imposed being consistent with the average heat flow in the Croatian part of the PBS (LENKEY et al., 2002; HORVÁTH et al., 2015). Similarly to the fluid flow, the Cauchy BC reproduces a heat flux through the boundary depending on: i) the difference between the reference and the calculated temperature values, and ii) a transfer-rate coefficient (DIERSCH, 2014). The reference temperature was set to 10 °C following the value imposed for the Dirichlet BC, while the transfer rate was calculated as the λ of the Q unit (Table 1) divided by its thickness.

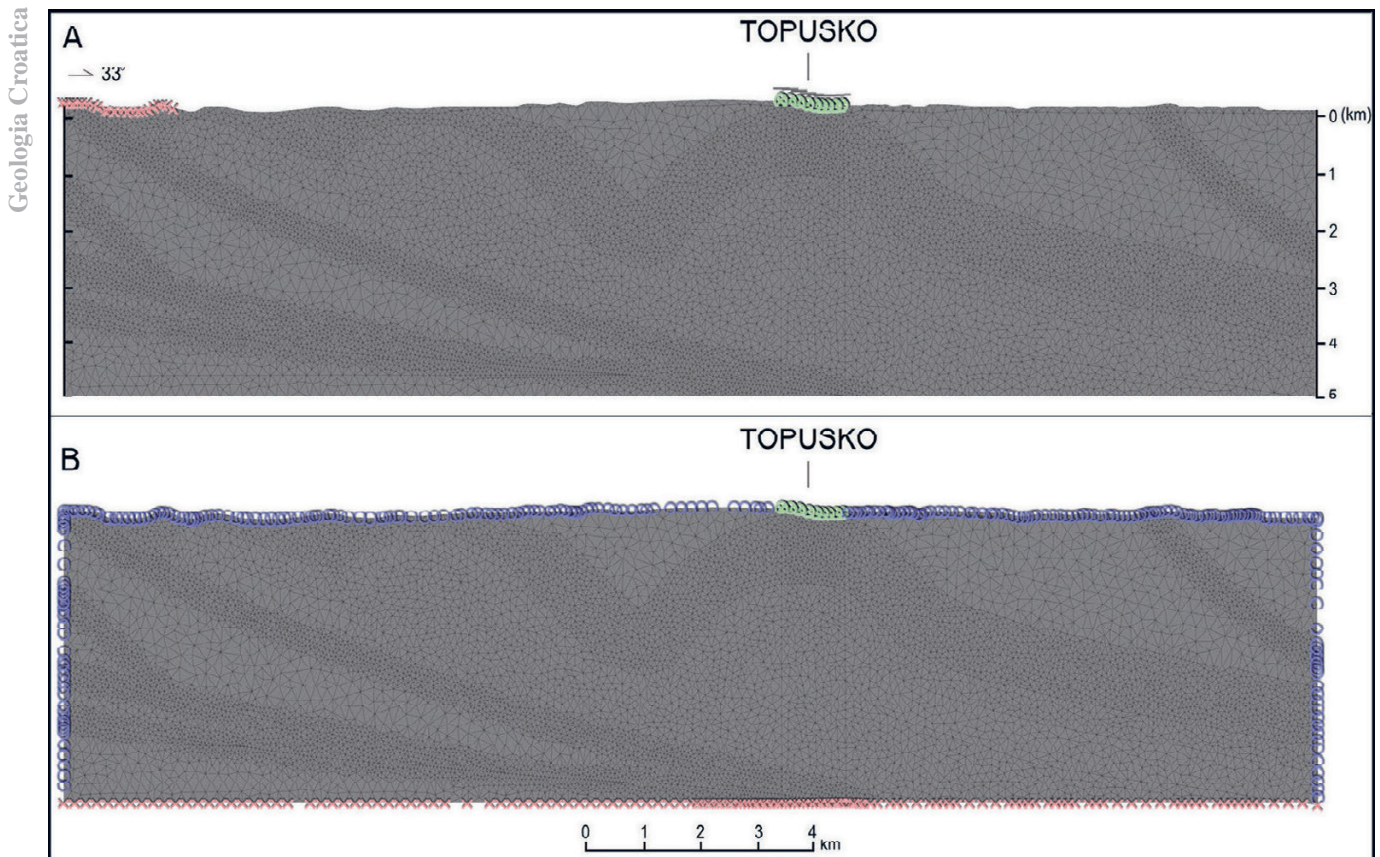


Figure 7. Fluid flow (A) and heat transport (B) boundary conditions (BCs) in the THS numerical model. Blue circles – 1st kind (Dirichlet) BC; Red crosses – 2nd kind (Neumann) BC; Green circles with crosses – 3rd kind (Cauchy) BC. Horizontal and vertical scale ratio is 1:1.

The THS numerical modelling was conducted performing transient state numerical simulations that account for the variations of the hydraulic head and temperature distributions over time. Therefore, it is important to set appropriate initial conditions for these variables achieving a better convergence of the numerical solution at the initial stages of the simulation. The initial value of the hydraulic head was set as 122 m, corresponding to the hydraulic head imposed at the fluid flow Cauchy BC. The initial distribution of the temperature was obtained through a steady-state simulation using: i) the described set of hydrogeological and thermal parameters for the hydrostratigraphic units (Table 1), ii) a 1st kind (Dirichlet) BC with a constant temperature value of 10 °C at the top of the domain, and iii) a 2nd kind (Neumann) BC at the bottom with

imposed inflow of 100 mW/m². The resulting temperature distribution reproduces a regional geothermal gradient of 35.8 °C/km, being consistent with available regional values in the study area (30 – 40 °C/km; MACENIĆ et al., 2020).

3.2.3. Simulation results

The best simulation of the THS was conducted employing the described set of hydrogeological and thermal parameters for the hydrostratigraphic units (Table 1) and the imposed boundary and initial conditions (Fig. 7). The transient simulation was run for 100 kyr obtaining a quasi-stationary distribution of the primary variables. This condition reproduces the long-term natural state of the hydrothermal system (i.e., GARG et al., 2007; KAISER et al., 2013; HAVRIL et al., 2016;

Table 1. Hydrogeological and thermal parameters assigned to the hydrostratigraphic units in the THS numerical model.

Unit	Age	Lithology	Thick [m]	K [m s ⁻¹]	Ss [m ⁻¹]	φ [%]	λ [W m ⁻¹ K ⁻¹]	ρc [MJ m ⁻³ K ⁻¹]
Q	Quaternary	Gravel, sand, silt	90	1*10 ⁻⁴	1*10 ⁻⁴	20	1.6	1.3
N	Neogene	Sand, clay, silt, marls	< 2,000	2*10 ⁻⁷	1*10 ⁻⁴	5	1.8	1.6
J	Jurassic	Magmatic-sedimentary ophiolitic complex	750 – 1,600	2*10 ⁻¹⁰	3.3*10 ⁻⁷	5	2	2.2
T _{2,3}	Middle-Upper Triassic	Limestone, dolostone	400 – 1,200	2*10 ⁻⁶	3.3*10 ⁻⁷	10	2.5	2.52
T ₁	Lower Triassic	Sandstone, marl, limestone, dolomite	600	2*10 ⁻⁹	3.3*10 ⁻⁷	5	2	1.6
P	Permian-Triassic	Siliciclastic rocks	650	2*10 ⁻¹¹	3.3*10 ⁻⁷	5	3	2.1
B	Palaeozoic	Schists shales, sandstones, conglomerates with limestone and dolomite lenses	2,000 – 3,000	2*10 ⁻¹²	3.3*10 ⁻⁷	2	3.5	2.1

Note: K: Hydraulic conductivity (DOMENICO & SCHWARTZ, 1997; FETTER, 2001; PAVIĆ et al., 2023); φ: Porosity (DOMENICO & SCHWARTZ, 1997); λ: Thermal conductivity (CERMAK & RYBACH, 1982, RMAN & TÓTH (2011), MÁDL-SZÓNYI & TÓTH (2015), STYLIANOU et al., 2016, BOROVIĆ et al., 2018; STOBER & BUCHER, 2021); Ss: specific storativity (DOMENICO & SCHWARTZ, 1997); ρc: volumetric heat capacity (LALLOUI & ROTTA LORIA, 2020)

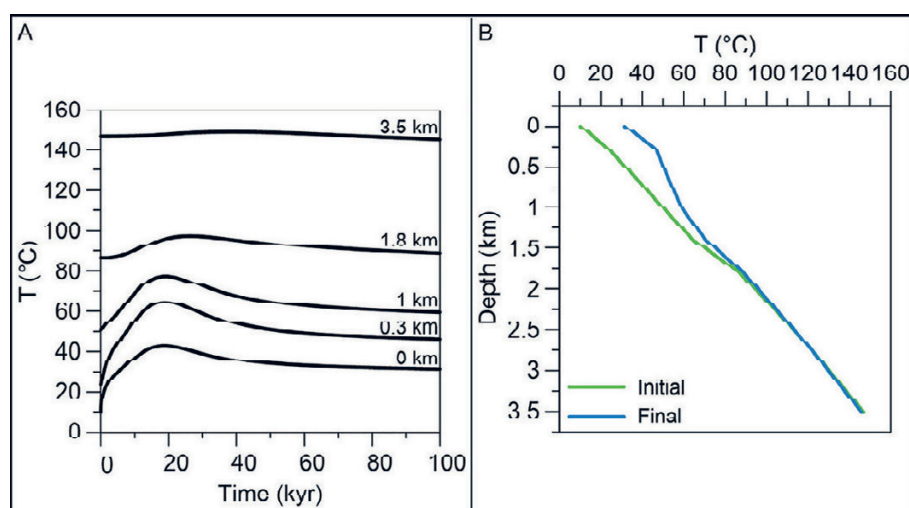


Figure 8. Modelled temperature variations over time (A) and final temperature distribution (B) in the Topusko area.

BOROVIĆ et al., 2019; POLA et al., 2020; TORRESAN et al., 2022), which is the goal of the THS numerical modelling.

The temperature variations over time at different depths in the subsurface of Topusko are represented in Fig. 8A. The simulated temperature gradually increases from the initial distribution reaching maximum values between 18 and 30 kyr depending on the considered depth. The temperature at the surface peaks to 42.6 °C at 18 kyr (initial value of 10 °C; depth = 0 km in Figs. 8A and 8B), while it reaches the maximum value of 77.4 °C at the same simulation time at base of the aquifer (initial value of 55.8 °C; depth = 1 km in Figs. 8A and 8B). The temperature differential progressively decreases with depth, being up to 2 °C in the deeper part of the modelling domain (depth = 3.5 km). After this increasing phase, the simulated temperatures progressively decrease. The final modelled temperatures at the surface and base of the aquifer are 31.3 °C and 59.5 °C (Figs. 8A and 8B), respectively, depicting a drop of 11.3 °C and 17.9 °C, respectively. The drop from the peak value decreases with the depth as well and is 3 °C in the deeper part of the modelling domain. Despite these variations, a practically constant temperature distribution is observed between 80 and 100 kyr with a maximum variation of 1.4 °C at the aquifer base. This result suggests that a quasi-stationary state of the solution was achieved.

The regional and local scale spatial distributions of temperature at the end of the simulation period (Figs. 9A and 9B, respectively) were further detailed. The temperature distribution within the aquifer at both regional and local scales exhibits significant spatial variability. In particular, a decrease from the initial values up to 14 °C is observed in the recharge area of the system where the infiltration of cold waters (10 °C as imposed by the Dirichlet BC for heat transport) occurs. Similar behaviour is observed in the recharge area of regional, topographically-driven groundwater systems (i.e., DOMENICO & PALCIAUSKAS, 1973; ANDERSON, 2005; AN et al., 2015). However, the temperature within the aquifer (pink polygon in Fig. 9) is up to 25 °C (depth of 0.7 km) as expected in shallow carbonate aquifers. The temperature in the aquifer progressively decreases eastward as depicted by the 20 °C isotherm located at a depth of approx. 1.6 km in the

central part of the modelling domain. This decrease is connected to the deep circulation of the infiltrated waters in the aquifer driven by both the topographic gradient and the deepening of the strata to the SW of Topusko (Fig. 6). The temperature increases in the hinge zone of the Topusko anticline where the upwelling of the thermal water favours the rise of the isotherms toward the surface (Fig. 9B). In particular, the isotherm of 35 °C is located approx. at the top of aquifer (depth of 0.1 km), while the isotherm 50 °C approaching to the water temperature of the Topusko thermal springs is located at a depth of 0.4 km. The modelled temperature is: i) up to 44 °C in the central part of the thermal anomaly at the depth investigated by the thermal wells in Topusko (0.2 km), ii) between 56 and 74 °C at the base of the aquifer, and iii) between 80 and 100 °C at the base of the T₁ hydrostratigraphic unit, which represents the semi-confining unit at the bottom of the aquifer (depth of approx. 1.8 km; Fig. 9).

The circulation of the fluid is generally directed from the recharge area of the model to the outflow area in Topusko. The flow mostly occurs in the T_{2,3} hydrostratigraphic unit where an average Darcy velocity of 0.18 m/yr (5.02×10^{-4} m/d) is modelled. It drops to 0.01 m/yr (2.9×10^{-5} m/d) in the T₁ and P hydrostratigraphic units at the bottom of the aquifer, and to 3.91×10^{-7} m/yr (1.07×10^{-9} m/d) in the impervious basement (B hydrostratigraphic unit). The direction and velocity of the flow in the aquifer show different distributions from the recharge to the outflow area depending on the K value of the hydrostratigraphic unit and the thickness of the aquifer. In the recharge area, the flow is almost horizontal with an average Darcy velocity of 0.27 m/yr (7.3×10^{-4} m/d). The velocity in the recharge area shows a high variability spanning over almost three orders of magnitude (minimum and maximum of 7.06×10^{-4} m/yr to 1.77 m/yr, respectively). In particular, the highest values are observed NE of the R3 fault (Fig. 6), where the thickness of the aquifer decreases (Fig. 9A) due to the anticline between the R3 and R4 faults. In the flow-through part of the system, the flow (average velocity of 0.17 m/yr corresponding to 4.54×10^{-4} m/d) is generally downward following the deepening of the aquifer to the SW of Topusko and resulting in the local drop of the isotherms (as depicted by

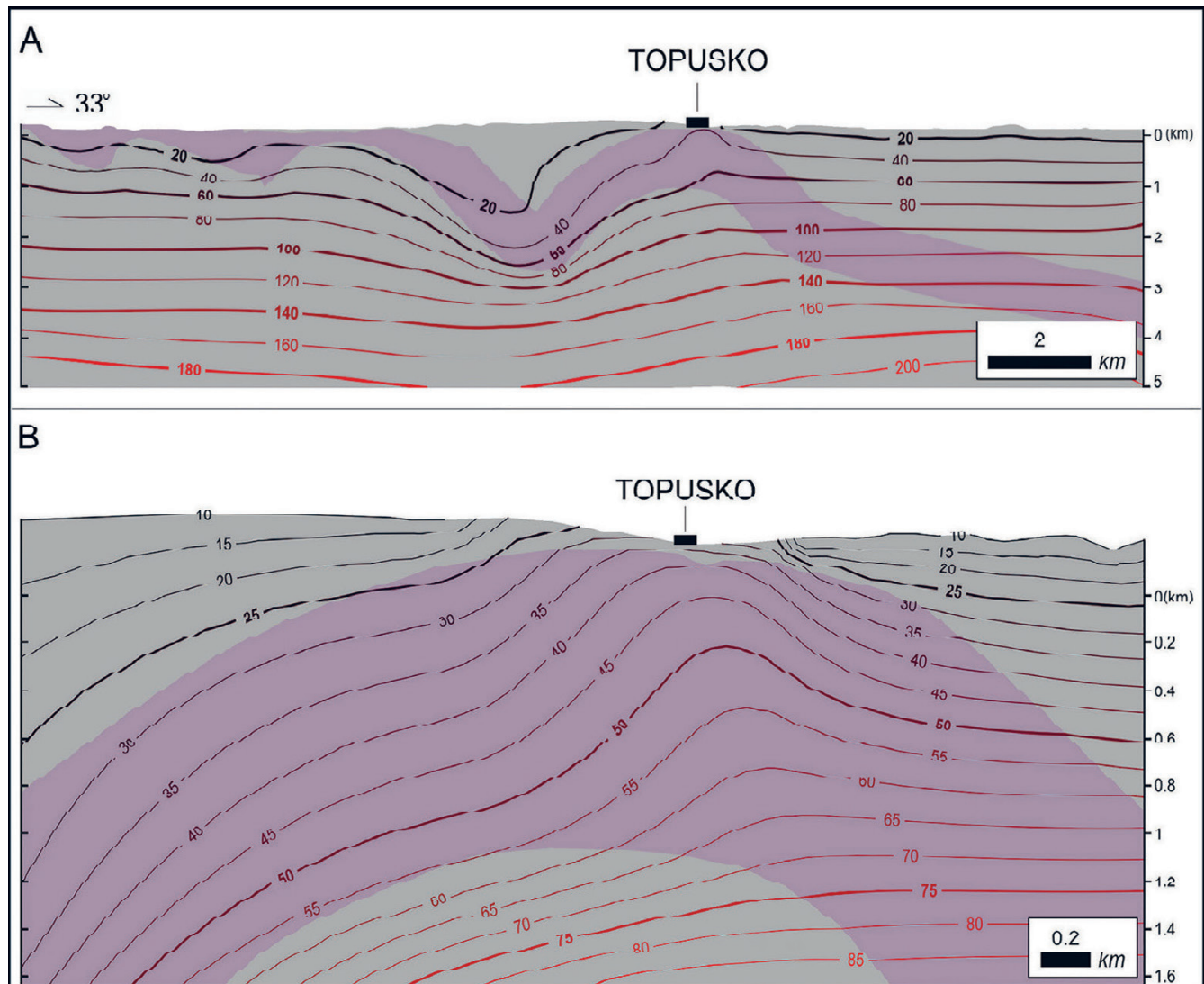


Figure 9. Regional temperature distribution in the modelling domain (A) and in the hinge zone of the Topusko anticline (B). A local temperature anomaly in the Topusko subsurface occurs reaching values of up to 74 °C at the base of the THS carbonate aquifer (pink polygon). The horizontal and vertical scale ratio is 1:1.

the 20 °C isotherm; Fig. 9A). The flow is generally upward in the southern limb of the Topusko anticline, but with similar magnitudes of the horizontal and vertical components of the Darcy velocity (average value of 0.15 m/yr corresponding to 4.16×10^{-4} m/d). In the Topusko area, the flow is upward and with a prevalent vertical component of the Darcy velocity. The average velocity value is of 0.13 m/yr (3.5×10^{-4} m/d), being slightly lower than the values observed in other parts of the aquifer, but the velocity field is more evenly distributed with minimum and maximum values of 1.21×10^{-3} and 0.28 m/yr, respectively. The Darcy velocity increases up to 0.28 m/yr in the upper part of the aquifer (i.e., the depth investigated by the thermal wells in Topusko) pointing to the quick rise of the thermal waters in the final part of the circulation path. The outflow modelled by the 3rd kind (Cauchy) BC is 0.18 m³/yr.

4. DISCUSSION

The Topusko hydrothermal system area is located at the tectonic boundary between the External and Internal Dinarides in the vicinity of the Sava suture zone (SCHMID et al., 2020). The Palaeozoic-Mesozoic terrains in the study area experi-

enced a complex polyphase tectonic evolution through the Cretaceous-Paleogene and the Neogene-Quaternary, which resulted in tectonic overprints of both regional shortening and extension. Observable regional shortening is associated with several NW-striking low-angle thrust faults and reverse faults (Fig. 4) that were probably formed due to the Cretaceous-Paleogene Adria Microplate and European Foreland collision (SCHMID et al., 2020). This regional NE – SW oriented shortening (TOMLJENOVIĆ & CSONTOS, 2001; SCHMID et al., 2008; USTASZEWSKI et al., 2008) resulted in the tectonic uplift of the Petrova gora Mt. and the formation of a folded system that also incorporates the Topusko anticline (Fig. 6). The polyphase tectonic history is further evidenced by structural reactivations of these faults and their tectonic inversions, which is observable in the tectonically inverted normal faults R3 and R4 (Fig. 4) indicating a NE – SW extension in the THS area. According to TOMLJENOVIĆ & CSONTOS (2001), NE – SW stretching of the inherited structures within the Croatian part of the PBS occurred during the Early-Middle Miocene due to back-arc type extension. Tectonic rejuvenation of the THS area through N – S regional contraction is observable at

the outcrop scale, with evidence of re-folding processes and mapped reverse faults within the Pliocene-Quaternary clastic sequence (e.g., USTASZEWSKI et al., 2008; HERAK et al., 2009; HERAK & HERAK, 2023).

The interpretation of the geological profiles constructed in this study suggests that the most used THS conceptual model (ŠIMUNIĆ, 2008) was based on an out-dated geological reconstruction. Furthermore, Šimunić's model was not constructed using a series of structural-geological profiles and a detailed reconstruction of subsurface relationships, but only spatial distribution of the lithological units. These shortcomings hindered the detailed understanding of complex subsurface relationships in the Topusko area. The new structural-geological interpretation was combined with geochemical and hydrogeological data (PAVIĆ et al., 2023, 2024) to propose a novel conceptual model of the THS. This model suggests that the THS is an intermediate-scale, gravity-driven, tectonically – controlled, hydrothermal system hosted in a Middle-Upper Triassic carbonate rock complex. The thermal water is of meteoric origin infiltrating approx. 13 km to the S of Topusko, where an area with intense karstification depicted by a high density of sinkholes occurs (Fig. 5). These sinkholes play a significant role in facilitating the diffuse recharge of the THS aquifer. Our interpretation in general coincides with BAĆ & HERAK's (1962) hypothesis, which identifies Middle and Upper Triassic carbonate deposits as the aquifer units facilitating deep groundwater circulation. They proposed that the thermal aquifer receives recharge from the Glina river headwaters, where Triassic carbonates are exposed, with a primary regional flow direction from S to N, aligning with our findings regarding the recharge area S of Topusko. Regional folded structures favour both the deep circulation of the infiltrated water, warming due to increased heat flow of the PBS (HORVÁTH et al., 2015), and the upwelling of the thermal water in the Topusko area. Fault and fracture systems in the hinge zone of the Topusko anticline promote the fracturing of the bedrock, the increase of the permeability field in the aquifer, and the quick rise of the thermal water from the deeper part of the reservoir. The extensional regime in the anticline hinge zone, combined with cogenetic fault and fracture systems and their permeable damage zones (PAVIĆ et al., 2023), creates a synergistic effect. This synergy enhances the overall permeability field in the discharge area, leading to the formation of abundant natural thermal springs.

The physical validity of the THS model was constrained conducting variable-density numerical simulations of fluid flow and heat transport. The numerical model was populated using a set of hydrogeological and thermal parameters from both the literature and field datasets. Boundary conditions were imposed at the borders of the modelling domain following the conceptual model of the THS. The best simulation was run for 100 kyr developing a local increase of the temperature distribution in the subsurface of Topusko (Fig. 9). In particular, the modelled temperatures were 31.3 and 44 °C at the surface and at the depth investigated by wells in Topusko, respectively. Despite these values are approx. 20 °C lower than the observed temperatures at the same depths, they can be considered as acceptable due to the simplifications imposed during the con-

struction of the numerical model. The thermal aquifer was reproduced using an equivalent porous medium approach, which assigns homogeneous values of the hydrogeological properties, while localised highly permeable damage zones channelling the outflow of the thermal water were not considered. The implementation of such structures in the numerical model would increase the fluid flow promoting the local increase of the temperature. In addition, a temperature between 80 and 100 °C was modelled in the semi-confining unit at the bottom of the aquifer being comparable with the reservoir temperature of 90 °C calculated with geothermometers. As discussed for the surficial temperature, the effect of localised highly permeable fault zones was not included in the conducted numerical model. These areas could favour the raising of the isotherms in the deeper part of the reservoir resulting in the higher temperature values calculated with geothermometers.

The simulated temperature distribution at the local scale reproduced the field values and was almost constant during the final 20 kyr of the simulation time (Fig. 8A). This result suggested that a quasi-stationary condition reproducing the natural state of the THS was achieved for a time span that is almost twice the mean residence time of the Topusko thermal water. The simulation results indicate a predominant groundwater flow pattern towards the Topusko discharge area. They also highlight the significant influence of the hydraulic conductivity field on groundwater flow patterns within the system. The modelled Darcy velocities ranged from 0.13 m/yr (Topusko) to 0.27 m/yr (recharge area) in the aquifer and decreased within the hydrostratigraphic units below it, directly reflecting the contrasting hydraulic conductivity values of different hydrostratigraphic units. This emphasises the importance of incorporating accurate K data into groundwater flow models for reliable predictions. An outflow of 0.18 m³/yr was modelled in the Topusko area, reproducing the thermal springs. Historical data on the flow rate of the springs before the drilling of the wells are not available and a more detailed numerical model would be needed to reproduce the effect of exploitation of the thermal water. The localised thermal anomaly in the anticline hinge zone corroborates the structural-causative processes enhancing fluid flow and heat transfer in the Topusko subsurface. Therefore, the results of the numerical modelling corroborate the validity of the conceptual model of the THS. In order to constrain the processes favouring the development of the modelled temperature distribution, the Rayleigh number (Ra) was calculated following the procedure described in TURCOTTE & SCHUBERT (1982). Ra is a dimensionless parameter indicating the threshold for the onset of free convection occurring when it exceeds the critical value of approximately 40 (TURCOTTE & SCHUBERT, 1982; NIELD & BEJAN, 1999; PESTOV, 2000; MÁDL-SZŐNYI & TÓTH, 2015). Considering the thickness of the reservoir (approx. 1 km) and its hydrogeological and thermal parametrisations, the conditions for the development of convection cells in the THS predominantly exist in the more permeable hinge zones of the Topusko anticline (Ra = 5,500 – 8,600 at temperature range simulated in the aquifer). Conduction is the predominant heat transfer mechanism in the rest of the THS aquifer (Ra < 60).

The used modelling approach proved to be a valuable initial step for understanding regional hydrogeological systems despite its simplifications. The lack of extensive boreholes or geophysical data limits the understanding of the regional geological and hydrogeological settings. Complex modelling with such limited data can lead to numerous assumptions, increasing the uncertainty of the simulations. Therefore, a simple numerical approach with a detailed hydrogeological and thermal parameterisation or robust geological reconstruction is initially preferable to reduce uncertainty. In the absence of a local dataset of hydrogeological and thermal properties, the parameterisation of hydrostratigraphic units in THS was conducted considering relevant regional studies and literature collections. Incorporating well-documented information from the literature enhanced the credibility and robustness of the model, facilitating a more comprehensive understanding of the hydrothermal system's dynamics. As fluid flow and heat transport are three-dimensional processes, the use of a 2D profile in the conducted THS representation is likely the most important simplification. This approach does not account for the proper local and regional characterisation of faults and related subsidiary structures, which are critical for fluid flow in fractured rocks. In the wider area of the THS, a dome-like anticline structure affects the geological and structural architecture in the subsurface, as illustrated in the presented profiles (Fig. 4, profiles THS-1-3). Describing this complex geological setting with the 2D model is inherently problematic, as it fails to capture the total spatial variability and structural-geological intricacies. This limitation adds to the discrepancies observed between modelled and actual temperatures and fluid flows, emphasising the need for more sophisticated modelling approaches capable of accounting for the geological complexity of the THS. The construction of a 3D model, supported by a more extensive dataset of hydrogeological, structural-geological, and thermal parameters, could improve the understanding of the thermal system dynamics. Considering the 3D geological architecture will significantly enhance the accuracy and reliability of future numerical simulations. Future investigations will focus on conducting a comprehensive 3D geological reconstruction of the subsurface based on detailed structural-geological and geophysical investigations that are necessary to characterise and justify the proposed local and regional structural-geological setting of the THS. This consequently includes the reconstruction of regional and local fault meshes for a more sophisticated numerical model.

5. CONCLUSION

The presented study utilised structural-geological field investigations and numerical modelling to develop a novel conceptual model of the THS. By constructing new geological profiles and integrating them with hydrogeological and geochemical data, we were able to provide new insights into the THS dynamics proposing a novel conceptual model. The recharge area of THS lies S of Topusko, where Triassic carbonates crop out. Regional and local scale fold and fault systems favour the deep circulation of the thermal water and the upwelling in Topusko forming a valuable geothermal resource.

Numerical modelling corroborates the proposed conceptual model of the THS. A local temperature anomaly was simulated in the Topusko subsurface reproducing the temperature field observations. The occurrence of such a localised thermal anomaly in the hinge zone of the Topusko anticline suggests an enhanced fluid flow and heat transport pointing to the impact of terrestrial heat flow and local geological structures on the system. In particular, the synergetic effect of the anticline hinge, which was determined by structural investigations, and cogenetic fault/fracture systems, which were identified by surface geophysical research, results in an enhanced permeability field in the discharge area, thereby enabling the formation of abundant natural thermal springs.

This study both advances the understanding of the THS and highlights the importance of integrating field observations with numerical modelling to physically validate and refine conceptual models. This integrated approach permits a more detailed reconstruction of the hydrogeological and thermal processes driving the development of geothermal resources. These aspects are crucial for developing site-specific exploitation plans of the resource, favouring its long-term utilisation.

ACKNOWLEDGEMENT

This research was funded by the Croatian Science Foundation (HRZZ), grant number UIP-2019-04-1218.

REFERENCES

- ANDERSON, M.P. (2005): Heat as a Ground Water Tracer.– *Groundwater*, 43/6, 951–968. doi: 10.1111/j.1745-6584.2005.00052.x
- ANDERSON, M., WOESSNER, W. & HUNT, R. (2015): *Applied Ground Water Modeling: Simulation of Flow and Advective Transport*.– Elsevier, London, 533 p.
- AN, R., JIANG, X.-W., WANG, J.-Z., WAN, L., WANG, X.-S. & LI, H. (2015): A theoretical analysis of basin-scale groundwater temperature distribution.– *Hydrogeol. J.*, 23/2, 397–404. doi: 10.1007/s10040-014-1197-y
- BAĆ, J. & HERAK, M. (1962): Prijedlog određivanja užih i širih zaštitnih zona termomineralnih izvora u Hrvatskoj [*Recommendation for determination of wider and narrow protection zones for thermo-mineral springs in Croatia* – in Croatian].– Unpublished report, Institute for geological research, Zagreb, 147 p.
- BAHUN, S. & RALJEVIĆ, B. (1969): Mineralna, termalna i ljekovita vrela [*Mineral and Thermal Springs* – in Croatian].– Unpublished report, Institute for geological research, Zagreb.
- BÉKÉSI, E., LENKEY, L., LIMBERGER, J., PORKOLÁB, K., BALÁZS, A., BONTÉ, D., VRIJLANDT, M., HORVÁTH, F., CLOETINGH, S. & VAN WEES, J.D. (2018): Subsurface temperature model of the Hungarian part of the Pannonian Basin.– *Global and Planetary Change*, 171, 48–64. doi: 10.1016/j.gloplacha.2017.09.020
- BENČEK, Đ., BUKOVAC, J., MAGAŠ, N. & ŠIMUNIĆ, A. (2014): Osnovna geološka karta Republike Hrvatske 1:100.000, List Karlovac L33-92 [*Basic Geological Map of the Republic of Croatia 1:100.000, Karlovac sheet* – in Croatian].– Croatian Geological Survey, Zagreb.
- BENČEK, Đ., BUKOVAC, J., MAGAŠ, N. & ŠIMUNIĆ, A. (2014): Osnovna geološka karta Republike Hrvatske 1:100.000, Tumač za list Karlovac L33-92 [*Basic Geological Map of the Republic of Croatia 1:100.000, Explanatory notes for Karlovac sheet* – in Croatian].– Croatian Geological Survey, Zagreb, 85 p.
- BOROVIĆ, S., MARKOVIĆ, T., LARVA, O., BRKIĆ, Ž. & MRAZ, V. (2016): Mineral and Thermal Waters in the Croatian Part of the Pannonian Ba-

- sin.– In: PAPIĆ, P. (ed.): Mineral and Thermal Waters of Southeastern Europe. Springer, Cham.
- BOROVIĆ, S., URUMOVIĆ, K., TERZIĆ, J. & PAVIČIĆ, I. (2018): Examining thermal conductivities of shallow subsurface materials for ground source heat pump utilization in the Pannonian part of Croatia.– The Mining-Geological-Petroleum Engineering Bulletin, 33/5, 27–35. doi: 10.17794/rgn.2018.5.3
- BOROVIĆ, S., POLA, M., BAČANI, A. & URUMOVIĆ, K. (2019): Constraining the recharge area of a hydrothermal system in fractured carbonates by numerical modelling.– Geothermics, 82, 128–149. doi: 10.1016/j.geothermics.2019.05.017
- BRÜCKL, E., BEHM, M., DECKER, K., GRAD, M., GUTERCH, A., KELLER, G.R. & THYBO, H. (2010): Crustal structure and active tectonics in the Eastern Alps.– Tectonics, 29/2. <https://doi.org/10.1029/2009TC002491>
- BUNDSCHUH, J. & CÉSAR SUÁREZ, A.M. (2010): Introduction to the Numerical Modeling of Groundwater and Geothermal Systems.– CRC Press, London. 522 p. doi: 10.1201/b10499
- BUKOVAC, J., ŠUŠNJAR, M., POLJAK, M. & ČAKALO, M. (1984): Osnovna geološka karta SFRJ 1:100.000, List Črnomelj L33–91 [*Basic Geological Map of the Republic of Croatia, 1:100.000, Črnomelj sheet* – in Croatian].– Federal Geological Survey, Belgrade.
- CALCAGNO, P., BAUJARD, C., GUILLOU-FROTIER, L., DAGALLIER, A. & GENTER, A. (2014): Estimation of the deep geothermal potential within the Tertiary Limagne basin (French Massif Central): An integrated 3D geological and thermal approach.– Geothermics, 51, 496–508. doi: 10.1016/j.geothermics.2014.02.002
- CERMAK, V., & RYBACH, L. (1982): Thermal properties: Thermal conductivity and specific heat of minerals and rocks.– In: ANGENEISTER, G. (ed.): Landolt-Börnstein: Zahlenwerte und Funktionen aus Naturwissenschaften und Technik, Neue Serie, Physikalische Eigenschaften der Gesteine. Springer Verlag, Berlin, Heidelberg and New York, V/1a, 305–343.
- CLOETINGH, S., CORNU, T., ZIEGLER, P.A., BEEKMAN, F. & ENTEC Working Group (2006): Neotectonics and intraplate continental topography of the northern Alpine Foreland.– Earth. Sci. Rev., 74, 127–196. doi: 10.1016/j.earscirev.2005.06.001
- CRITTENDEN, J.C., TRUSSELL, R.R., HAND, D.W., HOWE, K.J. & TCHOBANOGLOUS, G. (2012): MWH's Water Treatment.– John Wiley & Sons, Inc. doi: 10.1002/9781118131473
- CSONTOS, L. & VÖRÖS, A. (2004): Mesozoic plate tectonic reconstruction of the Carpathian region.– Palaeogeogr. Palaeoclimatol. Palaeoecol., 210/1, 1–56. doi: 10.1016/j.palaeo.2004.02.033
- D'AGOSTINO, N., AVALLONE, A., CHELONI, D., D'ANASTASIO, E., MANTENUTO, S. & SELVAGGI, G. (2008): Active tectonics of the Adriatic region from GPS and earthquake slip vectors.– Journal of Geophysical Research: Solid Earth, 113/B12. <https://doi.org/10.1029/2008JB005860>
- DHMZ. (2021): Monthly values and extremes.– Državni Hidrometeorološki Zavod [*Croatian Meteorological and Hydrological Service* – in Croatian]. (retrieved January 18, 2021) from https://meteo.hr/klima.php?section=klima_podaci¶m=k2_1
- DIERSCH, H.J.G. (2014): FEFLOW: Finite Element Modeling of Flow, Mass and Heat Transport in Porous and Fractured Media.– Springer Berlin, Heidelberg. doi: 10.1007/978-3-642-38739-5
- DI NAPOLI, R., MARTORANA, R., ORSI, G., AIUPPA, A., CAMARDA, M., DE GREGORIO, S., GAGLIANO CANDELA, E., LUZIO, D., MESSINA, N., PECORAINO, G. et al. (2011): The Structure of a Hydrothermal System from an Integrated Geochemical, Geophysical, and Geological Approach: The Ischia Island Case Study.– Geochem. Geophys. Geosyst., 12/7. <https://doi.org/10.1029/2010GC003476>
- DOMENICO, P.A. & SCHWARTZ, F.W. (1997): Physical and Chemical Hydrogeology (2nd edition).– Wiley, New York. 506 p.
- DOMENICO, P. A. & PALCIAUSKAS, V. V. (1973): Theoretical Analysis of Forced Convective Heat Transfer in Regional Ground-Water Flow.– GSA Bulletin, 84/12, 3803–3814. doi: 10.1130/0016-7606(1973)84<3803:TAO FCH>2.0.CO;2
- EVANS, M.A. & FISCHER, M.P. (2012): On the distribution of fluids in folds: A review of controlling factors and processes.– J. Struct. Geol., 44, 2–24. doi: 10.1016/j.jsg.2012.08.003
- FABBRI, P., POLA, M., PICCININI, L., ZAMPIERI, D., ROGHEL, A. & DALLA LIBERA, N. (2017): Monitoring, utilization and sustainable development of a low-temperature geothermal resource: A case study of the Euganean Geothermal Field (NE, Italy).– Geothermics, 70, 281–294. doi: 10.1016/j.geothermics.2017.07.002.
- FAULKNER, D. R., JACKSON, C. A. L., LUNN, R. J., SCHLISCHE, R. W., SHIPTON, Z. K., WIBBERLEY, C. A. J., & WITHJACK, M. O. (2010): A review of recent developments concerning the structure, mechanics and fluid flow properties of fault zones.– J. Struct. Geol., 32/11, 1557–1575. doi: 10.1016/j.jsg.2010.06.009
- FEDERAL GEOLOGICAL SURVEY. (1970): Geological Map of SFRY 1:500.000.– Federal Geological Survey, Beograd.
- FETTER, C.W. (2001): Applied Hydrogeology (4th edition).– Prentice Hall, Upper Saddle River, New Jersey.
- FLÓVENZ, Ó.G., HERSIR, G.P., SÆMUNDSSON, K., ÁRMANNSSON, H. & FRIDRIKSSON, T. (2012): Geothermal Energy Exploration Techniques.– In: SAYIGH, A. (ed.): Comprehensive Renewable Energy, 51–95. doi: 10.1016/B978-0-08-087872-0.00705-8
- FUCHS, S. & BALLING, N. (2016): Improving the temperature predictions of subsurface thermal models by using high-quality input data. Part 1: Uncertainty analysis of the thermal-conductivity parameterization.– Geothermics, 64, 42–54. doi: 10.1016/j.geothermics.2016.04.010
- GARG, S.K., PRITCHETT, J.W., WANNAMAKER, P.E. & COMBS, J. (2007): Characterization of geothermal reservoirs with electrical surveys: Beowawe geothermal field.– Geothermics, 36/6, 487–517. doi: 10.1016/j.geothermics.2007.07.005
- GHASEMIZADEH, R., HELLWEGER, F., BUTSCHER, C. et al. (2012): Review: Groundwater flow and transport modeling of karst aquifers, with particular reference to the North Coast Limestone aquifer system of Puerto Rico.– Hydrogeol. J., 20, 1441–1461. doi: 10.1007/s10040-012-0897-4
- GOLDSCHIEDER, N., MÁDL-SZŐNYI, J., ERŐSS, A. & SCHILL, E. (2010): Review: Thermal water resources in carbonate rock aquifers.– Hydrogeol. J., 18/6, 1303–1318. doi: 10.1007/s10040-010-0611-3
- GORJANOVIĆ-KRAMBERGER, D. (1905): Geologijske i hidrografijske prilike oko Topuskoga s obzirom na topuske terme [*Geological and hydrographic conditions in the area of Topusko with respect to thermal spring* – in Croatian].– Works of the Yugoslav Academy of Sciences and Arts – Mathematics and Science Division, 37, 2–34.
- GORJANOVIĆ-KRAMBERGER, D. (1917): Geologijske i hidrografijske prilike oko Topuskog s osobitim obzirom na Topuske terme [*Geological and hydrographic conditions in the area of Topusko with particular interest in thermal springs* – in Croatian].– Reports of discussions in Mathematics and Science Division, Yugoslav Academy of Sciences and Arts, Zagreb.
- GRENERCZY, G., SELLA, G.F., STEIN, S. & KENYERES, A., (2005): Tectonic implications of the GPS velocity field in the northern Adriatic region.– Geophys. Res. Lett., 32/16. doi: 10.1029/2005GL022947
- HAVRIL, T., MOLSON, J.W. & MÁDL-SZŐNYI, J. (2016): Evolution of fluid flow and heat distribution over geological time scales at the margin of unconfined and confined carbonate sequences - A numerical investigation based on the Buda Thermal Karst analogue.– Mar. and Pet. Geol., 78, 738–749. doi: 10.1016/j.marpetgeo.2016.10.001
- HEASLER, H.P., JAWOROWSKI, C. & FOLEY, D. (2009): Geothermal systems and monitoring hydrothermal features.– In: YOUNG, R. & NORBY, L. (eds.): Geological Monitoring. Geological Society of America, Boulder. doi:10.1130/2009.monitoring(05)
- HERAK, D., HERAK, M. & TOMLJENOVIĆ, B. (2009): Seismicity and earthquake focal mechanisms in North-Western Croatia.– Tectonophysics, 465/1–4, 212–220. doi: 10.1016/j.tecto.2008.12.005

- HERAK, M. & HERAK, D. (2023): Properties of the Petrinja (Croatia) earthquake sequence of 2020–2021 – Results of seismological research for the first six months of activity.– *Tectonophysics*, 858, 229885. doi: 10.1016/j.tecto.2023.229885
- HORVÁTH, F. & TARI, G. (1999): The IBS Pannonian basin project: A review of the main results and their bearings on hydrocarbon exploration.– *Geol. Soc. London Spec. Publ.*, 156, 195–213. doi: 10.1144/GSL.SP.1999.156.01.11
- HORVÁTH, F., BADA, G., SZAFIÁN, P., TARI, G., ÁDÁM, A. & CLOETINGH, S. (2006): Formation and deformation of the Pannonian Basin: Constraints from observational data.– *Geological Society Memoir*, 32, 191–206. doi: 10.1144/GSL.MEM.2006.032.01.11
- HORVÁTH, F., MUSITZ, B., BALÁZS, A., VÉGH, A., UHRIN, A., NÁDOR, A., KOROKNAI, B., PAP, N., TÓTH, T. & WÓRUM, G. (2015): Evolution of the Pannonian basin and its geothermal resources.– *Geothermics*, 53, 328–352. doi: 10.1016/j.geothermics.2014.07.009
- HOUNSLOW, A.W. (1995): *Water Quality Data: Analysis and Interpretation* (1st ed.).– CRC Press. doi: 10.1201/9780203734117
- HRVATOVIĆ, H. (2005): *Geological Guidebook through Bosnia and Herzegovina*.– Geological Survey Sarajevo-Geology Department, 163 p.
- KAISER, B.O., CACACE, M., & SCHECK-WENDEROTH, M. (2013): 3D coupled fluid and heat transport simulations of the Northeast German Basin and their sensitivity to the spatial discretization: different sensitivities for different mechanisms of heat transport.– *Environ. Earth Sci.*, 70/8, 3643–3659. doi: 10.1007/s12665-013-2249-7
- KASTELIC, V. & CARAFA, M.M.C. (2012): Fault slip rates for the active External Dinarides thrust-and-fold belt.– *Tectonics*, 31/3. doi: 10.1029/2011TC003022
- KHODAYAR, M. & BJÖRNSSON, S. (2024): Conventional Geothermal Systems and Unconventional Geothermal Developments: An Overview.– *Open J. Geol.*, 14/2, 196–246. doi: 10.4236/ojg.2024.142012
- KOROLIJA, B., ŽIVALJEVIĆ, T. & ŠIMUNIĆ, A. (1980): Osnovna geološka karta SFRJ 1:100.000, List Slunj L 33–104 [*Basic Geological Map of SFRJ 1:100.000, Slunj sheet* – in Croatian].– Institute for Geological Research, Zagreb, Geological Survey, Sarajevo; Federal Geological Survey, Belgrade.
- KOROLIJA, B., ŽIVALJEVIĆ, T. & ŠIMUNIĆ, A. (1981): Osnovna geološka karta SFRJ 1:100.000, Tumač za list Slunj L33–104 [*Basic Geological Map of SFRJ 1:100.000, Explanatory notes for Slunj sheet* – in Croatian].– Institute for geological research, Zagreb; Geological survey, Sarajevo; Federal geological survey: Belgrade.
- KOSOVIC, I., BRIŠKI, M., PAVIĆ, M., PADOVAN, B., PAVIČIĆ, I., MATOŠ, B., POLA M. & BOROVIĆ, S. (2023): Reconstruction of Fault Architecture in the Natural Thermal Spring Area of Daruvar Hydrothermal System Using Surface Geophysical Investigations (Croatia).– *Sustainability*, 15/16, 12134. doi: 10.3390/su151612134
- KOSOVIC, I., MATOŠ, B., PAVIČIĆ, I., POLA, M., MILEUSNIĆ, M., PAVIĆ, M. & BOROVIĆ, S. (2024): Geological modeling of a tectonically controlled hydrothermal system in the southwestern part of the Pannonian basin (Croatia).– *Front. Earth Sci.*, 12. doi: 10.3389/feart.2024.1401935
- LALOU, L. & ROTTA LORIA, A. F. (2020): Heat and mass transfers in the context of energy geostructures.– In: *Analysis and Design of Energy Geostructures*. Academic Press., 69–135. doi: 10.1016/B978-0-12-816223-1.00003-5
- LEI, H. & ZHU, J. (2013): Numerical modeling of exploitation and reinjection of the Guantao geothermal reservoir in Tanggu District, Tianjin, China.– *Geothermics*, 48, 60–68. doi: 10.1016/j.geothermics.2013.03.008
- LENKEY, L., DÖVÉNYI, P., HORVÁTH, F. & CLOETINGH, S.A.P.L. (2002): Geothermics of the Pannonian basin and its bearing on the neotectonics.– In: CLOETINGH, S.A.P.L., HORVÁTH, F., BADA, G. & LANKREIJER, A.C. (eds.): *EGU Stephan Mueller Special Publication Series*, 3, 29–40. doi: 10.5194/smsps-3-29-2002
- MACENIĆ, M., KUREVIJA, T. & MEDVED, I. (2020): Novel geothermal gradient map of the Croatian part of the Pannonian basin system based on data interpretation from 154 deep exploration wells.– *Renew. Sustain. Energy Rev.*, 132. doi: 10.1016/J.RSER.2020.110069
- MÁDL-SZÖNYI, J. & TÓTH, Á. (2015): Basin-scale conceptual groundwater flow model for an unconfined and confined thick carbonate region.– *Hydrogeol. J.*, 23/7, 1359–1380. doi: 10.1007/s10040-015-1274-x
- MAJER, V. (1978): Stijene “dijabaz-spilit-keratofirske asocijacije” u području Abez-Lasinja u Pokuplju i Baniji (Hrvatska, Jugoslavija) [*Rocks of diabase-spilite-keratophyre association in the area of Abez-Lasinja in Pokuplje and Banije (Croatia, Yugoslavia)* – in Croatian].– *Acta Geol.*, 9/4, 42, 137–158.
- MAJER, V. (1993): Ofiolitni kompleks Banije s Pokupljem u Hrvatskoj i Pastirevo u Bosni [*Ophiolite complexes of Banija and Pokuplje in Croatia and Pastirevo in Bosnia* – in Croatian].– *Acta Geol.*, 23/2, 39–84.
- MANDAL, A., BASANTARAY, A.K., CHANDROTH, A. & MISHRA, U. (2019): Integrated Geophysical Investigation to Map Shallow Surface Alteration/Fracture Zones of Atri and Tarabalo Hot Springs, Odisha, India.– *Geothermics*, 77, 24–33. doi: 10.1016/j.geothermics.2018.08.007
- MARINI, L. (2000): *Geochemical techniques for the exploration and exploitation of geothermal energy*.– Dipartimento per lo Studio del Territorio e delle sue Risorse, Università degli Studi di Genova, Italy.
- MARTINSEN, G., BESSIERE, H., CABALLERO, Y., KOCH, J., COLLADOS-LARA, A. J., MANSOUR, M., SALLASMAA, O., PULIDO-VELAZQUEZ, D., WILLIAMS, N.H., ZAADNOORDIJK, W.J. & STIENSEN, S. (2022). Developing a pan-European high-resolution groundwater recharge map – Combining satellite data and national survey data using machine learning.– *Science of the Total Environment*, 822 p. doi: 10.1016/j.scitotenv.2022.153464
- MAZOR, E. (2004): *Chemical and Isotopic Groundwater Hydrology*, 3rd ed.– Marcel Dekker, New York, 13–179 p.
- MOECK, I.S. (2014): Catalog of geothermal play types based on geologic controls.– *Renewable and Sustainable Energy Reviews*, 37, 867–882. doi: 10.1016/j.rser.2014.05.032
- MONTANARI, D., MINISSALE, A., DOVERI, M., GOLA, G., TRUMPY, E., SANTILANO, A. & MANZELLA, A. (2017): Geothermal resources within carbonate reservoirs in western Sicily (Italy): A review.– *Earth-Science Reviews*, 169, 180–201. doi: 10.1016/j.earscirev.2017.04.016
- MROCZEK, E.K., MILICICH, S.D., BIXLEY, P.F., SEPULVEDA, F., BERTRAND, E.A., SOENGGONO, S. et al. (2016): Ohaaki geothermal system: Refinement of a conceptual reservoir model.– *Geothermics*, 59, 311–324. doi: 10.1016/j.geothermics.2015.09.002
- MUFFLER, P. & CATALDI, R. (1978): Methods for regional assessment of geothermal resources.– *Geothermics*, 7/2–4, 53–89. doi: 10.1016/0375-6505(78)90002-0
- NIELD, D.A. & BEJAN, A. (1999): *Convection in Porous Media* (2nd Edition).– Springer, New York. doi:10.1007/978-1-4757-3033-3
- OJHA, L., KARUNATILLAKE, S., KARIMI, S. & BUFFO, J. (2021): Amagmatic hydrothermal systems on Mars from radiogenic heat.– *Nat. Commun.*, 12/1. doi: 10.1038/s41467-021-21762-8
- PAVELIĆ, D. (2001): Tectonostratigraphic model for the North Croatian and North Bosnian sector of the Miocene Pannonian Basin System.– *Basin Res.*, 13, 359–376. doi: 10.1046/j.0950-091x.2001.00155.x
- PAVELIĆ, D., KOVAČIĆ, M., MIKNIĆ, M., AVANIĆ, R., VRSALJKO, D., BAKRAČ, K., TIŠLJAR, J., GALOVIĆ, I. & BORTEK, Ž. (2003): The Evolution of the Miocene Environments in the Slavonian Mts. Area (Northern Croatia).– In: VLAHOVIĆ, I. & TIŠLJAR, J. (eds.): 22nd IAS Meeting of Sedimentology – Opatija 2003, Field Trip Guidebook. Croatian Geological Survey, Zagreb.
- POLA, M., CACACE, M., FABBRI, P., PICCININI, L., ZAMPIERI, D. & TORRESAN, F. (2020): Fault Control on a Thermal Anomaly: Conceptual and Numerical Modeling of a Low-Temperature Geothermal System in the Southern Alps Foreland Basin (NE Italy).– *J. Geophys. Res. Solid Earth*, 125/5, e2019JB017394, doi: 10.1029/2019JB017394
- PAVIĆ, M., KOSOVIC, I., POLA, M., URUMOVIĆ, K., BRIŠKI, M., & BOROVIĆ, S. (2023): Multidisciplinary Research of Thermal Springs Area in Topusko (Croatia).– *Sustainability*, 15/6, 5498. doi: 10.3390/su15065498
- PAVIĆ, M., BRIŠKI, M., POLA, M., & BOROVIĆ, S. (2024): Hydrogeochemical and environmental isotope study of Topusko thermal waters, Cro-

- atia.– Environ. Geochem. Health, 46/4, 133. doi: 10.1007/s10653-024-01904-9
- POURASKARPARAST, Z., AGHAEI, H., COLOMBERA, L., MASOERO, E. & GHAEDI, M. (2024): Fracture aperture: A review on fundamental concepts, estimation methods, applications, and research gaps.– Mar. Pet. Geol., 164, 106818. doi: 10.1016/j.marpetgeo.2024.106818
- PRELOGOVIĆ, E., SAFTIĆ, B., KUK, V., VELIĆ, J., DRAGAŠ, M. & LUČIĆ, D. (1998): Tectonic activity in the Croatian part of the Pannonian basin.– Tectonophysics, 297/1–4, 283–293. doi: 10.1016/S0040-1951(98)00173-5
- RMAN, N. & TÓTH, G. (2011): Hydrogeological conceptual model.– Geological Survey of Slovenia, Ljubljana; Geological Institute of Hungary, Budapest [in Hungarian], 25 p.
- RMAN, N. (2014): Analysis of long-term thermal water abstraction and its impact on low-temperature intergranular geothermal aquifers in the Mura-Zala basin, NE Slovenia.– Geothermics, 51, 214–227. doi: 10.1016/j.geothermics.2014.01.011
- RMAN, N., BĀLAN, L.L., BOBOVEČKI, I., GĀL, N., JOLOVIĆ, B., LAPANJE, A. et al. (2020): Geothermal sources and utilization practice in six countries along the southern part of the Pannonian basin.– Environ. Earth Sci., 79, 1–12. doi: 10.1007/s12665-019-8746-6
- ROYDEN, L.H., & HORVÁTH, F. (1988): The Pannonian Basin: A Study in Basin Evolution.– American Association of Petroleum Geologists. doi: 10.1306/M45474
- SAFTIĆ, B., VELIĆ, J., SZTANO, O., JUHASZ, G. & IVKOVIĆ, Ž. (2003): Tertiary Subsurface Facies, Source Rocks and Hydrocarbon Reservoirs in the SW Part of the Pannonian Basin (Northern Croatia and South-Western Hungary). Geologia Croatica, 56/1, 101–122. doi:10.4154/232
- SCANLON, B., & DUTTON, A. (2000): Groundwater Recharge in Texas.– The University of Texas at Austin, and Marios Sophocleous, Kansas Geological Survey, Lawrence, KS.
- SCANLON, B.R., MACE, R.E., BARRETT, M.E. & SMITH, B. (2003): Can we simulate regional groundwater flow in a karst system using equivalent porous media models? Case study, Barton Springs Edwards aquifer, USA.– Journal of Hydrology, 276/1–4, 137–158. doi: 10.1016/S0022-1694(03)00064-7
- SCHMID, S.M., BERNOULLI, D., FÜGENSCHUH, B., MATENCO, L., SCHEFER, S., SCHUSTER, R., TISCHLER, M. & USTASZEWSKI, K. (2008): The Alpine-Carpathian-Dinaridic orogenic system: Correlation and evolution of tectonic units.– Swiss J. Geosci., 101, 139–183. doi: 10.1007/s00015-008-1247-3
- SCHMID, S. M., FÜGENSCHUH, B., KOUNOV, A., MAŢENCO, L., NIEVERGELT, P., OBERHÄNSLI, R., PLEUGER, J., SCHEFER, S., SCHUSTER, R., TOMLJENOVIĆ, B., USTASZEWSKI, K. & VAN HINSBERGEN, D.J.J. (2020): Tectonic units of the Alpine collision zone between Eastern Alps and western Turkey.– Gondwana Research, 78, 308–374. doi: 10.1016/j.gr.2019.07.005
- STEVANOVIĆ, Z., DULIĆ, I. & DUNČIĆ, M. (2015): Some experiences in tapping deep thermal waters of the Triassic karstic aquifer in the Pannonian Basin of Serbia.– Central European Geology, 58/1–2, 50–61. doi: 10.1556/24.58.2015.1-2.3
- STYLIANOU, I., TASSOU, S., CHRISTODOULIDES, P., PANAYIDES, I. & FLORIDES, G. (2016): Measurement and analysis of thermal properties of rocks for the compilation of geothermal maps of Cyprus.– Renewable Energy, 88, 418–429. doi:10.1016/j.renene.2015.10.058
- SZANYI, J. & KOVÁCS, B. (2010): Utilization of geothermal systems in South-East Hungary.– Geothermics, 39/4, 357–364. doi: 10.1016/j.geothermics.2010.09.004
- ŠEGOTIĆ, B. & ŠMIT, I. (2007): Studija optimirane energetske učinkovitosti korištenja geotermalnih voda [Study of Optimized Energy Efficiency of Geothermal Water Use – in Croatian].– Unpublished report, Termoinženjering-projektiranje, Zagreb.
- ŠIKIĆ, K. (1990): Osnovna geološka karta Republike Hrvatske 1:100.000, list Bosanski Novi L 33–105 [Basic Geological Map of the Republic of Croatia 1:100.000, Bosanski Novi sheet – in Croatian].– Croatian Geological Survey, 2014.
- ŠIKIĆ, K. (1990): Osnovna geološka karta Republike Hrvatske 1:100.000, Tumač za list Bosanski Novi L 33-70 [Basic Geological Map of the Republic of Croatia 1:100.000, Explanatory notes for Bosanski Novi sheet – in Croatian].– Croatian Geological Survey Zagreb, 2014.
- ŠIMUNIĆ, A. (2008): Topusko.– In: ŠIMUNIĆ, A. & HEĆIMOVIĆ, I. (eds.): Geotermalne i mineralne vode Republike Hrvatske [Mineral and Thermal Waters of the Republic of Croatia – in Croatian]. Croatian Geological Survey, Zagreb.
- TARI, G., DÖVÉNYI, P., DUNKL, I., HORVÁTH, F., LENKEY, L., STEFANESCU, M., SZAFIÁN, P. & TÓTH, T. (1999): Lithospheric structure of the Pannonian basin derived from seismic, gravity and geothermal data.– Geol. Soc. London Spec. Publ., 156, 215–250. doi: 10.1144/GSL.SP.1999.156.01.12
- TEUTSCH, G. & SAUTER, M. (1991): Groundwater modeling in karst terranes: Scale effects, data acquisition and field validation.– In: Third conference on hydrogeology, ecology, monitoring, and management of ground water in Karst Terranes.– National Ground Water Association, Dublin, Ohio, 17–35.
- TOMLJENOVIĆ, B. & CSONTOS, L. (2001): Neogene–Quaternary structures in the border zone between Alps, Dinarides and Pannonian Basin (Hrvatsko zagorje and Karlovac Basins, Croatia).– Int. J. Earth Sci., 90/3, 560–578. doi: 10.1007/s005310000176
- TOMLJENOVIĆ, B. (2002): Strukturne značajke Medvednice i Samoborskog gorja [Structural features of Medvednica and Samobor hills – in Croatian].– Unpubl. PhD Thesis, Faculty of Mining, Geology and Petroleum Engineering, University of Zagreb, Zagreb.
- TOMLJENOVIĆ, B., CSONTOS, L., MÁRTON, E. & MÁRTON, P. (2008): Tectonic evolution of the northwestern Internal Dinarides as constrained by structures and rotation of Medvednica Mountains, North Croatia.– Geol. Soc. London Spec. Publ., 298/1, 145–167. doi: 10.1144/SP298.8
- TORRESAN, F., PICCININI, L., CACACE, M., POLA, M., ZAMPIERI, D. & FABBRI, P. (2022): Numerical modeling as a tool for evaluating the renewability of geothermal resources: the case study of the Euganean Geothermal System (NE Italy).– Environ. Geochem. Health, 44/7, 2135–2162. doi: 10.1007/s10653-021-01028-4
- TÓTH, J. (2009): Gravitational systems of groundwater flow: theory, evaluation, utilization.– Cambridge University Press, Cambridge. doi: 10.1017/CBO9780511576546
- TURCOTTE, D.L. & SCHUBERT, G. (1982): Geodynamics: Applications of continuum mechanics to geological problems.– Wiley, New York, 464 p.
- USTASZEWSKI, K., SCHMID, S. M., FÜGENSCHUH, B., TISCHLER, M., KISSLING, E. & SPAKMAN, W. (2008): A map-view restoration of the Alpine-Carpathian-Dinaridic system for the early Miocene.– Swiss J. Geosci., 101/Suppl 1, 273–294. doi: 10.1007/s00015-008-1288-7
- USTASZEWSKI, K., KOUNOV, A., SCHMID, S. M., SCHALTEGGER, U., KRENN, E., FRANK, W. & FÜGENSCHUH, B. (2010): Evolution of the Adria-Europe plate boundary in the northern Dinarides: From continent-continent collision to back-arc extension.– Tectonics, 29/6. doi: 10.1029/2010TC002668
- USTASZEWSKI, K., HERAK, M., TOMLJENOVIĆ, B., HERAK, D. & MAŢEJ, S. (2014): Neotectonics of the Dinarides-Pannonian Basin transition and possible earthquake sources in the Banja Luka epicentral area.– J. Geodyn., 82, 52–68. doi: 10.1016/j.jog.2014.04.006
- VASS, I., TÓTH, T.M., SZANYI, J. & KOVÁCS, B. (2018): Hybrid numerical modelling of fluid and heat transport between the overpressured and gravitational flow systems of the Pannonian Basin.– Geothermics, 72, 268–276. doi: 10.1016/j.geothermics.2017.11.013
- VELIĆ, I. & SOKAČ, B. (1982): Novi nalaz naslaga donjeg i srednjeg trijasa u zapadnom Kordunu (središnja Hrvatska) [New discoveries of the Lower and Middle Triassic in the western part of Kordun area (central Croatia) – in Croatian].– Geološki vjesnik, 35, 47–57.
- VLAHOVIĆ, I., TIŠLJAR, J., VELIĆ, I. & MATIČEC, D. (2005): Evolution of the Adriatic Carbonate Platform: Palaeogeography, main events and depositional dynamics.– Palaeogeogr. Palaeoclimatol. Palaeoecol., 220/3–4, 333–360. doi: 10.1016/j.palaeo.2005.01.011

WORTHINGTON, S.R.H., FOLEY, A.E., & SOLEY, R.W.N. (2019): Transient characteristics of effective porosity and specific yield in bedrock aquifers.– *J. Hydrol.*, 578, 124129. doi: 10.1016/j.jhydrol.2019.124129

XIONG, J., LIN, H., DING, H., PEI, H., RONG, C. & LIAO, W. (2020): Investigation on thermal property parameters characteristics of rocks and its

influence factors.– *Natural Gas Industry B*, 7/3, 298–308. doi: 10.1016/j.ngib.2020.04.001

URL 1: <https://www.avenza.com/avenza-maps/>. Accessed on 29 April, 2024.

URL 2: <https://www.esri.com/news/arcnews/spring12articles/introducing-arcgis-101.html>. Accessed on 29 April, 2024.